

Revisiting Graph Neural Networks for Graph-level Tasks: Taxonomy, Empirical Study, and Future Directions

Haoyang Li¹, Yuming Xu¹, Alexander Zhou¹, Yongqi Zhang²

¹The Hong Kong Polytechnic University, Hong Kong SAR, China

²Hong Kong University of Science and Technology, Hong Kong SAR, China

haoyang-comp.li@polyu.edu.hk, martin.xu@connect.polyu.hk, alexander.zhou@polyu.edu.hk, yongqizhang@hkust-gz.edu.cn

Abstract

Graphs are fundamental data structures for modeling complex interactions in domains such as social networks, molecular structures, and biological systems. Graph-level tasks, which involve predicting properties or labels for entire graphs, are crucial for applications like molecular property prediction and subgraph counting. While Graph Neural Networks (GNNs) have shown significant promise for these tasks, their evaluations are often limited by narrow datasets, task coverage, and inconsistent experimental setups, hindering their generalizability. In this paper, we present a comprehensive experimental study of GNNs on graph-level tasks, systematically categorizing them into five types: node-based, hierarchical pooling-based, subgraph-based, graph learning-based, and self-supervised learning-based GNNs. To address these challenges, we propose a unified evaluation framework OpenGLT for graph-level GNNs. OpenGLT standardizes the evaluation process across diverse datasets, multiple graph tasks (e.g., classification and regression), and real-world scenarios, including noisy, imbalanced, and few-shot graphs. Extensive experiments are conducted on 16 baseline models across five categories, evaluated on 13 graph classification and 13 graph regression datasets. These experiments provide comprehensive insights into the strengths and weaknesses of existing GNN architectures.

Keywords

Graph Neural Networks, Graph-level tasks, Unified evaluation

1 Introduction

Graphs represent objects as nodes and their relationships as edges, which are key data structures across various domains to model complex interactions [7, 23, 24], such as social networks, molecular structures, biological systems, etc. Early graph representation learning methods [19, 33, 77, 89] laid the foundation of graph learning. Graph-level tasks aim at predicting properties of an entire graph, rather than individual nodes or edges. These tasks are crucial in domains including subgraph counting in database management [27, 56], molecular property prediction in chemistry [39, 117], and protein classification in bioinformatics [53, 71]. Recently, graph neural networks (GNNs) [14, 60, 63, 65, 83, 95, 100] have emerged as powerful tools for graph-structured and anomaly detection tasks [68]. They learn node representations by iteratively aggregating neighbor information to obtain graph representations.

Depending on the approach, we categorize GNNs for graph-level tasks into five categories: node-based, hierarchical pooling

(HP)-based, subgraph-based, graph learning (GL)-based, and self-supervised learning (SSL)-based methods. Node-based GNNs [35, 48, 88, 101] compute node representations through message passing and aggregate them via a permutation-invariant readout function, such as averaging, to form the final graph embedding. HP-based GNNs [6, 16, 59, 70] apply pooling operations to reduce the graph size and capture hierarchical structure, yielding multi-level graph representations. Subgraph-based GNNs [4, 18, 76, 102] divide the graph into subgraphs, learn a representation for each, and then aggregate these to represent the whole graph. GL-based GNNs [25, 54, 61, 116] enhance graph quality by reconstructing structure and features. SSL-based GNNs [44, 53, 84, 86, 97] pretrain on unlabeled data, either by predicting graph properties or maximizing agreement between augmented views of the same graph.

Although various GNNs have been designed for graph-level tasks, their evaluations are often restricted to a narrow range of domain-specific datasets and insufficient baseline comparisons [22, 62, 94, 116]. To ensure fair comparison, we identify and address three key shortcomings in current evaluation frameworks.

- **Issue 1. No clear taxonomy for GNNs on graph-level Tasks.** Graph-level tasks require different approaches than node-level tasks, yet a clear taxonomy for GNNs on graph-level tasks is lacking. This gap hinders holistic understanding and systematic comparison of models.
- **Issue 2. Restricted Coverage of GNN Architectures.** Most evaluations focus on a limited set of architectures, such as node-based GNNs, while often ignoring more expressive models like subgraph-based GNNs. This narrow coverage limits performance comparisons and overlooks the strengths of diverse approaches.
- **Issue 3. Insufficient Data Diversity.** Current evaluations typically use datasets from a narrow range of domains, such as chemistry or biology. This limited diversity can lead to overfitting and restricts the generalizability of GNNs to other domains like social networks or different types of graphs.
- **Issue 4. Narrow Task and Scenario Scope.** Current evaluation frameworks typically focus on a single type of graph-level task, such as molecular graph classification, and overlook diverse applications like cycle or path counting. They also assume access to ample clean labeled data, neglecting real-world challenges such as noise, class imbalance, or limited labeled graphs.
- **Issue 5. Inconsistent Evaluation Pipelines.** The lack of a standardized evaluation pipeline results in inconsistent comparisons. Different works often use varying data splits, tuning protocols, and evaluation metrics, hindering fair assessment of model performance. A unified evaluation framework is needed for transparent and reliable comparisons.

To address these five issues, we introduce OpenGLT, a comprehensive framework designed to provide a fair and thorough assessment of GNNs for graph-level tasks. We begin by systematically categorizing existing GNNs for graph-level tasks into five distinct types and conduct an in-depth analysis of each type to understand their unique strengths and limitations. Next, we introduce a unified evaluation pipeline with standardized data splitting and experimental settings. This pipeline incorporates graph datasets from diverse domains, including biology, chemistry, social networks, and motif graphs, ensuring broad and representative evaluations. Furthermore, we comprehensively evaluate the effectiveness and efficiency of existing graph-level GNNs on both graph classification and graph regression tasks, such as cycle counting. Beyond standard tasks, we also evaluate GNNs in real-world scenarios, including noisy graphs, imbalanced datasets, and few-shot learning settings. This unified framework ensures a holistic and equitable evaluation of GNNs, promoting fair comparisons and advancing their applicability across various graph-level tasks.

We summarize the contributions of this paper on graph-level benchmarking as follows.

- We systematically revisit GNNs for graph-level tasks and categorize them into five types, with in-depth analysis in Section 3.
- We propose a unified open-source evaluation framework, OpenGLT, which covers diverse tasks, datasets, and scenarios.
- We conduct extensive experiments on 13 graph classification and 13 graph regression datasets, systematically comparing the effectiveness and efficiency of state-of-the-art GNNs, providing insights into their relative strengths, limitations, and directions.

2 Preliminaries and Related Work

In this section, we first introduce graph-level tasks and then review existing experimental studies related to these graph-level tasks. Important notations are summarized in Table 1.

2.1 Graph-level Tasks

Graphs are a fundamental data structure to model relations between nodes in real-world datasets. Consequently, graph-level tasks, including classification and regression, are widely applied across domains, such as recommendation systems in social networks [11, 64], molecular property and activity prediction in chemistry [9, 11, 32, 69, 72], and protein analysis, motif identification, or gene expression prediction in biology [74, 109]. Formally, we denote a graph as $G_i(V_i, A_i, X_i)$, where $V_i, A_i \in \{0, 1\}^{|V_i| \times |V_i|}$, $X_i \in \mathbb{R}^{|V_i| \times d_x}$, denote nodes, adjacency matrix, and node features, respectively. In general, graph-level tasks are to learn a mapping from G_i to a label (classification) or a continuous value (regression).

2.2 Related Works of Experimental Studies

As summarized in Table 2, existing benchmarks and surveys [22, 39, 58, 94, 116] often face four key limitations [22, 39, 58, 94, 116]: (i) a lack of systematic taxonomy for graph-level tasks; (ii) a predominant focus on node-based GNNs [20, 39, 71], leaving diverse architectures partially absent with poor categorization; (iii) the neglect of realistic scenarios such as noise, imbalance, and few-shot settings, which hinders robustness assessment; and (iv) a lack of comprehensive efficiency metrics for usability evaluation.

Table 1: Summary on important notations.

Symbols	Meanings
$G_i(V_i, A_i, X_i)$	The graph G_i
y_i	Discrete label or continuous value of G_i
$N_i^l(v), N_i(v)$	The l -hop and 1-hop neighbors of v in G_i
f_θ	GNN model
l, L	GNN layer index and the total layer number
$\mathbf{h}_i^{(l)}(v)$	The l -th layer representation of v in G_i
$\mathbf{m}_i^{(l)}(v)$	The l -th layer message aggregated intermediate for node v
e_{uv}	Edge feature of edge (u, v) in G_i
$\mathbf{h}_i(v)$	Final node representation of v in G_i
$\mathbf{H}_i^{(l)}(V_j)$	l -th layer representation of nodes V_j in G_i
$\mathbf{H}_i(V_j)$	Final representation of nodes V_j in G_i
READOUT(\cdot)	Graph-level aggregation function producing \mathbf{h}_i from node/cluster embeddings
\mathbf{h}_i	Graph representation of G_i
y_i^*	Prediction of GNN f_θ for G_i
$S_i^{(l)}$	Cluster assignment matrix at l -th layer
$\hat{G}_i^*(V_i, \hat{A}_i^*, \hat{X}_i^*)$	The reconstructed graph for G_i
\hat{G}_i, \hat{G}_i	Augmented positive views for G_i
$s(\mathbf{h}_i, \mathbf{h}_j)$	Similarity score between G_i and G_j
$\mathcal{L}_{task}(\cdot)$	Task loss (Equation (4))
$\mathcal{L}_{ssl}(\cdot)$	Self-supervised learning loss (Equation (11))
$\mathcal{L}_{cl}(\cdot)$	Contrastive learning loss (Equation (15))

3 Graph Neural Networks for Graph-level Tasks

Recently, GNNs [15, 31, 34, 41, 52, 81, 93, 111, 121] have emerged as powerful tools to learn node representations, due to their ability to capture complex relationships within graph structures. Existing GNNs for graph-level tasks can generally be categorized into five types: node-based, pooling-based, subgraph-based, graph learning-based, and self-supervised learning-based GNNs.

3.1 Node-based GNNs

As shown in Figure 1 (a), node-based GNNs first learn latent representations for individual nodes, which then are used to form a graph-level representation. Generally, each GNN f_θ consists of two fundamental operations, i.e., AGG(\cdot) and COM(\cdot) [35, 51], which can be parameterized by learnable matrices \mathbf{W}_{agg} and \mathbf{W}_{com} , respectively. Formally, given a graph $G_i(V_i, A_i, X_i)$ and a node $v \in V_i$, in the l -th layer, AGG($^{(l)}(\cdot)$) in Equation (1) first aggregates the hidden representation $\mathbf{h}_i^{(l-1)}(u)$ and edge representation \mathbf{e}_{uv} of each neighbor u of node v and obtain the aggregated result $\mathbf{m}_i^{(l)}(v)$. Subsequently, as shown in Equation (2), COM($^{(l)}(\cdot)$) combines the aggregated neighbor information $\mathbf{m}_i^{(l)}(v)$ and the latest information $\mathbf{h}_i^{(l-1)}(v)$ of node v to obtain the l -th layer graph-level representation $\mathbf{h}_i^{(l)}(v)$.

$$\mathbf{m}_i^{(l)}(v) = \text{AGG}^{(l)}\left(\{\mathbf{h}_i^{(l-1)}(u), \mathbf{e}_{uv} : u \in \mathcal{N}_i(v)\}\right) \quad (1)$$

$$\mathbf{h}_i^{(l)}(v) = \sigma\left(\text{COM}^{(l)}\left(\mathbf{h}_i^{(l-1)}(v), \mathbf{m}_i^{(l)}(v)\right)\right), \quad (2)$$

where σ denotes a non-linear function (e.g., ReLU [57]). $\mathbf{h}_i^{(0)}(v)$ is initialized as $X_i[v]$. After L layers aggregation, we can obtain node

Table 2: Summary of existing surveys and experimental studies on GNNs for graph-level tasks. Sur. and Exp. denote Survey and Experiments, respectively. Taxo. denotes Taxonomy, Subg. denotes Subgraph. Additionally, FewS., Imba., Effect., and Effic. denote Few-shot, Imbalanced, Effectiveness, and Efficiency, respectively.

Paper	Paper Type		Taxo.	GNN Type					Data Type				Scenarios			Eval Metric		
	Sur.	Exp.		Node	Pool	Subg.	GL	SSL	SN	BIO	CHE	MC	Clean	Noise	FewS.	Imba.	Effect.	Effic.
GNNS [99]	✓																	
TUD [71]		✓		✓					✓	✓	✓		✓					✓
OGB [39]		✓		✓						✓	✓		✓					✓
GNNB [20]		✓		✓		✓					✓		✓					✓
ReGCB [58]		✓		✓					✓	✓	✓		✓					✓
FGNNB [22]		✓		✓	✓				✓	✓	✓		✓					✓
GPB [94]		✓			✓							✓	✓					✓
OpenGLT	✓	✓	✓	✓	✓	✓	✓	✓	✓	✓	✓	✓	✓	✓	✓	✓	✓	✓

representations $\mathbf{H}_i(V_i) \in \mathbb{R}^{|V_i| \times d_H}$. Then, the graph representation \mathbf{h}_i of G_i can be summarized from the node representation $\mathbf{H}_i(V_i)$ by a READOUT function [53] as follows:

$$\mathbf{h}_i = \text{READOUT}(\mathbf{H}_i(V_i)), \quad (3)$$

where READOUT is a permutation-invariant function, such as AVERAGE, SUM, or MAX functions [53]. The SUM function as an example is $\mathbf{h}_i = \sum_{v \in V_i} \mathbf{H}_i(V_i)[v]$.

Model Optimization. Then, we can use a decoder (e.g., 2-layer Multi-Layer Perceptrons (MLPs) [119]) to predict discrete class or continuous property value for each graph G_i based \mathbf{h}_i . In summary, given the labeled training dataset $\mathcal{LG} = \{(G_i, y_i)\}_{i=1}^n$ and the prediction y_i^* for each graph G_i by the GNN f_θ , the GNN f_θ can be optimized by minimizing the task loss as follows:

$$\theta^* = \arg \min_{\theta} \frac{1}{|\mathcal{LG}|} \sum_{G_i \in \mathcal{LG}} \mathcal{L}_{task}(f_\theta, G_i, y_i). \quad (4)$$

$$s.t. \quad \mathcal{L}_{task}(y_i^*, y_i) = \begin{cases} -\sum_{y \in y_i} y \log y_i^*[y], & y_i \in \{0, 1\}^{|\mathcal{Y}|} \\ \|y_i^* - y_i\|_2, & y_i \in \mathbb{R} \end{cases} \quad (5)$$

3.2 Hierarchical Pooling-based GNNs

As shown in Figure 1 (b), hierarchical pooling (HP)-based GNNs are designed to capture hierarchical structures in the graph, which can reduce the graph size progressively while preserving its essential structural information. This is achieved by clustering nodes into groups and summarizing their features, allowing the model to focus on condensed graph structures and finally obtain the representation of each graph.

As mentioned in Equations (1) and (2), at the l -th layer, node-based GNNs learn node representations using the adjacency matrix \mathbf{A}_i and the node hidden representations $\mathbf{H}_i^{(l-1)}(V_i)$. In contrast, at the l -th layer, HP-based GNNs first generate a new cluster assignment matrix $\mathbf{S}_i^{(l)} \in \{0, 1\}^{n_{l-1} \times n_l}$, where $n_l < n_{l-1}$. This matrix maps the nodes $V_i^{(l-1)}$ from the $(l-1)$ -th layer to a cluster index in $\{1, \dots, n_l\}$. The new adjacency matrix $\mathbf{A}_i^{(l)} \in \mathbb{R}^{n_l \times n_l}$ is then reconstructed based on the cluster assignment matrix $\mathbf{S}_i^{(l)}$ as follows:

$$\mathbf{A}_i^{(l)} = \mathbf{S}_i^{(l)\top} \mathbf{A}_i^{(l-1)} \mathbf{S}_i^{(l)}. \quad (6)$$

Subsequently, n_l new nodes $V_i^{(l)}$ are created to represent the n_l clusters. Then, the node hidden representations $\mathbf{H}_i^{(l-1)}(V_i^{(l)})$ can

obtained by a READOUT operation on nodes each cluster $k \in \{1, \dots, n_l\}$ as follows:

$$\mathbf{H}_i^{(l-1)}(V_i^{(l)})[k] = \text{READOUT}(\mathbf{H}_i^{(l-1)}(V_i^{(l-1)})[V_k]), \quad (7)$$

where $V_k = \{u \mid \mathbf{S}_i^{(l)}[u][k] = 1\}$ are nodes in the cluster k .

Depending on the technique of generating the cluster matrix $\mathbf{S}_i^{(l)}$, existing pooling-based GNNs can be classified into three types.

- **Similarity-based.** Similarity-based approaches [16, 59, 70] cluster nodes based on the similarity of nodes features or structures. These methods rely on predefined similarity metrics such as cosine similarity of node features, or graph partitioning algorithms to generate the cluster assignment matrix. Graclus [16, 70] and CC-GNN [59] assign nodes to different clusters based on feature similarity and graph structure.
- **Node Dropping-based.** Node dropping-based methods [8, 30, 49] focus on reducing the number of nodes in the graph by learning an importance score for each node. Nodes with the highest scores are retained, while others are dropped, effectively shrinking the graph size in a controlled manner. TopKPool [8, 30] and SAGPool [49] aim to learn an importance score for each node and retain only the top- n_l nodes with the highest scores at layer l . In other words, they only assign one node for each cluster and directly drop the other nodes.
- **Learning-based.** Learning-based approaches [3, 6, 17, 87, 106] use neural network architectures to learn the cluster assignment matrix $\mathbf{S}_i^{(l)}$ based on the graph's node features and structure, which adaptively learn how to cluster nodes in a way that preserves the graph's essential information. Specifically, Diff-Pool [106] and MinCutPool [6] use non-linear neural networks and and GMT [3] use the multi-head attention mechanism [87], to learn a cluster matrix $\mathbf{S}_i^{(l)}$ based on the learned node features $\mathbf{H}_i^{(l-1)}$ and adjacent matrix $\mathbf{A}_i^{(l-1)}$. EdgePool [17] proposes to learn the edge score between each pair of connected nodes and then generate the cluster matrix accordingly.

3.3 Subgraph-based GNNs

Recent studies propose subgraph-based GNNs with enhanced expressive power, enabling them to more effectively capture substructure information. As shown in Figure 1 (c), the core idea is

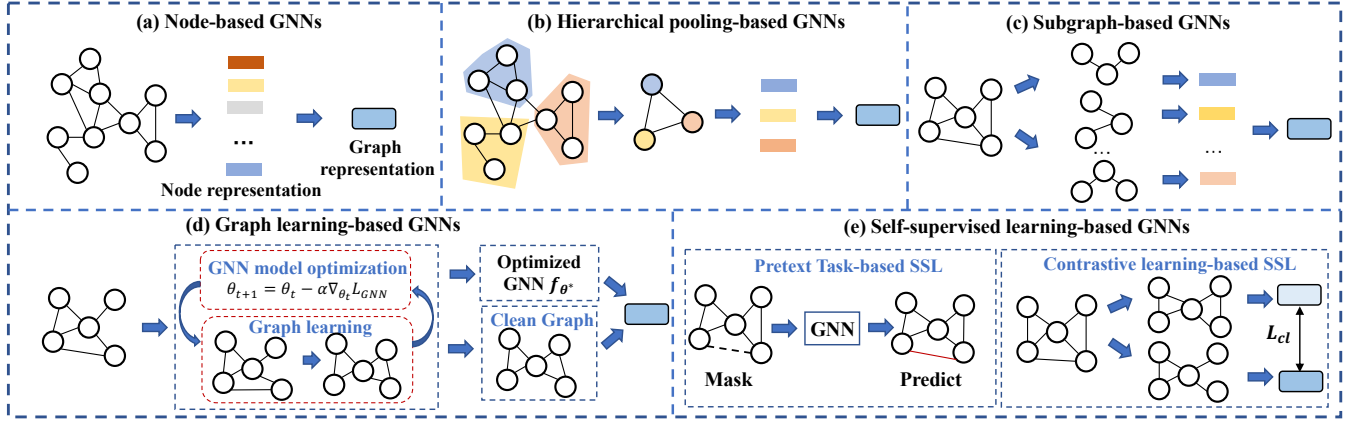


Figure 1: The five types of current GNNs for graph-level tasks.

to decompose the input graph into a set of overlapping or non-overlapping subgraphs and then learn representations for each subgraph to improve the final graph representation. Formally, given a graph $G_i(V_i, A_i, X_i)$, existing models first generate n_s subgraphs $G_{i,j}(V_{i,j}, A_{i,j}, X_{i,j})_{j=1}^{n_s}$. Then, for each subgraph $G_{i,j}$, the node representation of $v \in V_{i,j}$ is learned by Equations (1) and (2). In this approach, each node $v \in V_i$ can have multiple representations because it may appear in multiple sampled subgraphs. To derive the final node representation $\mathbf{h}_i(v)$, these representations are merged. A common approach is to use a READOUT function to combine them, as follows:

$$\mathbf{h}_i(v) = \text{READOUT}(\mathbf{h}_{i,j}(v) | v \in V_{i,j}). \quad (8)$$

Depending on the techniques of generating the subgraphs, current subgraph-based approaches can be classified into three types.

- **Graph Element Deletion-based.** These approaches [5, 13, 18, 75] propose deleting specific nodes or edges to create subgraphs, enabling GNNs to focus on the most informative parts of the graph by removing noise or less relevant elements. For example, DropGNN [75] and ESAN [5] generate subgraphs through random edge deletion to enhance model expressiveness. Conversely, SGOOD [18] abstracts a superstructure from the original graphs and applies sampling and edge deletion on this superstructure, thereby creating a more diverse graphs.
- **Rooted Subgraph-based.** These approaches [4, 29, 42, 76, 78, 102, 103, 107, 110, 114] focus on generating subgraphs centered around specific nodes, referred to as *root nodes*, with the aim of capturing the structural role and local topology of the root node within the subgraph. The primary motivation is to enhance the representational power of GNNs by encoding the root node's position within the subgraph, as well as its relationships to other nodes within the same subgraph. Specifically, I2GNN [42], ECS [102], and ID-GNN [107] propose to append side information to the root nodes or edges to capture the position information, such as an ID identifier for root nodes (e.g., the root v is 1 and other nodes are 0) [42, 107], and node degree and shortest distance information [102]. Also, NestGNN [110] and GNN-AK [114] use rooted subgraphs with different hops

to capture the hierarchical relationships within graphs for root nodes.

- **k -hop Subgraph-based.** Similar to rooted subgraph-based approaches [1, 26, 73, 80, 90, 104], k -hop subgraph-based approaches construct subgraphs based on the k -hop neighborhood of each node v , focusing on capturing the local structure around each node. Unlike rooted subgraph-based approaches, which aggregate information from 1-hop neighbors, k -hop subgraph-based approaches aggregate information not only from 1-hop neighbors but also directly from nodes up to k hops away. Specifically, MixHop [1] utilizes a graph diffusion kernel to gather multi-hop neighbors and computes the final representation. SEKGNN [104], KP-GNN [26], EGO-GNN [80], and k -hop GNN [73] progressively updates node representations by aggregating information from neighbors within k -hops. MAGNA [90] proposes to learn more accurate weights between each pair of nodes based on all the paths between them within k -hops.

3.4 Graph Learning-based GNNs

Due to uncertainty and complexity in data collection, real-world graphs often contain redundant, biased, or noisy edges and features. When operating on such imperfect structures, vanilla GNNs may learn spurious correlations and thus fail to produce reliable graph representations, ultimately leading to incorrect predictions. To mitigate this issue, as shown in Figure 1 (d), recent work [25, 61, 116] propose to learn from purified or reconstructed graph structure and enhanced node features that better reflect the underlying signal to improve the quality of the learned graph representations. Given a labeled graph set $\mathcal{LG} = \{(G_i, y_i)\}_{i=1}^n$, the graph learning-based approaches can be formulated as bi-level optimization problem.

$$\begin{aligned} \theta^* &= \min_{\theta \in \Theta} \frac{1}{|\mathcal{LG}|} \sum_{G_i \in \mathcal{LG}} \mathcal{L}_{task}(f_{\theta}, \hat{G}_i^*(V_i, \hat{A}_i^*, \hat{X}_i^*), y_i). \quad (9) \\ \text{s.t. } \hat{A}_i^*, \hat{X}_i^* &= \arg \min_{\hat{A}_i, \hat{X}_i} \mathcal{L}_{gl}(f_{\theta^*}, \hat{G}_i(V_i, \hat{A}_i, \hat{X}_i), y_i), \\ &\forall G_i \in \mathcal{G} \end{aligned} \quad (10)$$

At the low level in Equation (10), current approaches propose different graph learning objectives $\mathcal{L}_{gl}(\cdot)$ to reconstruct graph structure

A_i and node features X_i . Then, in Equation (9), $\hat{G}_i^*(V_i, \hat{A}_i^*, \hat{X}_i^*)$ will be used to optimize the GNNs by the loss function in Equation (4).

Depending on the techniques of reconstructing graphs, current GL-based GNNs can be categorized into three types.

- **Preprocessing-based.** Preprocessing-based approaches [21, 55, 98] reconstruct graphs and then use them to optimize GNNs directly. The basic idea is to first reveal the common graph patterns and modify the graph structure and node features to recover these patterns. For example, GNN-Jaccard [98] and GNAT [55] observe that similar nodes tend to be connected by edges. Therefore, they remove edges between dissimilar nodes and add edges between similar ones. Also, GNN-SVD [21] observes that noisy edges and node features tend to increase the rank of the adjacency matrix. Therefore, GNN-SVD reconstructs graphs by decreasing the rank of the adjacency matrix.
- **Jointly Training-based.** In contrast to static preprocessing-based methods, jointly training-based approaches aim to optimize the GNN while iteratively reconstructing the graph structure and node features alongside the GNN model parameters. This iterative bi-level optimization enables the GNN to dynamically adapt the graph structure and features based on task-specific objectives. For instance, several approaches [28, 46, 47, 54, 67, 85], such as ADGNN [54], ProGNN [47], and SimPGCN [46], propose reconstructing the edges between each pair of nodes by minimizing the GNN loss on the reconstructed structure while also reducing the rank of the adjacency matrix. Alternatively, several approaches [91, 112, 118], such as MOS-GSL [118] and HGP-SL [112], focus on first partitioning each graph into subgraphs based on node similarities and predefined motifs, and then reconstructing the edges between these subgraphs rather than at the individual node level.

3.5 Self Supervised Learning-based GNNs

Self-supervised learning (SSL) has become a powerful paradigm to pretrain GNNs without the need for labeled data, which can capture the node patterns and graph patterns. As shown in Figure 1 (e), the key idea of SSL approaches is to create supervised signals directly from the structure and node features of the unlabeled graph itself, leveraging the graph’s inherent properties to guide the learning process. Formally, given a set of unlabeled graphs $\mathcal{UG} = \{G_i(V_i, A_i, X_i)\}_{i=1}^{|\mathcal{UG}|}$, the GNN f_θ is pretrained as follows:

$$\theta' = \arg \min_{\theta} \frac{1}{|\mathcal{UG}|} \sum_{G_i \in \mathcal{UG}} \mathcal{L}_{ssl}(f_\theta, G_i, Signal_i), \quad (11)$$

where $Signal_i$ is the supervised signals from the unlabeled graph G_i and θ' is the optimized GNN parameters. Then, the pretrained $f_{\theta'}$ can be used to predict graph labels or properties. Formally, given the set of labeled graphs $\mathcal{LG} = \{G_j(V_j A_j, X_j), y_j\}_{j=1}^{|\mathcal{LG}|}$, the GNN $f_{\theta'}$ is optimized as follows:

$$\theta^* = \arg \min_{\theta'} \frac{1}{|\mathcal{LG}|} \sum_{G_j \in \mathcal{LG}} \mathcal{L}_{task}(f_{\theta'}, G_j, y_j), \quad (12)$$

where the task loss $\mathcal{L}_{task}(\cdot)$ is defined in Equation (4).

Depending on the specific technique used to auto-generate supervised signals from unlabeled graphs, SSL-based GNN approaches can be broadly categorized into two main paradigms.

- **Pretext Task-based.** Pretext task-based approaches [38, 40, 44, 45, 97, 109, 113] design auxiliary tasks to help the model learn useful representations from the graph structure and features without requiring external labels. Current approaches design diverse node-level and graph-level tasks to capture intrinsic graph patterns [97], such as predicting node attribute, node degree, and the node number. For example, HMGNN [109] pretrains GNNs by predicting the links between nodes and the number of nodes in each graph. MGSSL [113] first masks the edges among motifs and then predicts the missing edges. MoAMA [44] first masks node features and then uses GNNs to reconstruct the node features based on the masked graphs. GraphMAE [38] and GPTGNN [40] predict both node attributes and edges.
- **Graph Contrastive Learning-based.** Graph contrastive learning (GCL)-based GNNs [36, 50, 77, 84, 92, 108] aim to learn representations by contrasting positive and negative examples. The basic idea is to maximize the similarity between different views or augmentations of the same node or graph (positive pairs) while minimizing the similarity between different nodes or graphs (negative pairs). In such a way, GCL-based approaches can distinguish the similarity between nodes and graphs. In general, the SSL loss $\mathcal{L}_{ssl}(\cdot)$ in Equation (11) can be formulated as follows.

$$\theta' = \arg \min_{\theta} \frac{1}{|\mathcal{UG}|} \sum_{G_i \in \mathcal{UG}} \mathcal{L}_{cl}(f_\theta, \hat{G}_i, \tilde{G}_i, Neg_i). \quad (13)$$

$$s.t. \hat{G}_i, \tilde{G}_i = \arg \min_{\hat{G}_i, \tilde{G}_i} \mathcal{L}_{positive}(G_i, \mathcal{T}), \forall G_i \in \mathcal{UG}, \quad (14)$$

where $\mathcal{L}_{cl}(\cdot)$ is the contrastive loss. Additionally, $\mathcal{L}_{positive}(\cdot)$ denotes the view generation loss used to generate two positive views (i.e., \hat{G}_i and \tilde{G}_i for each graph G_i) where \mathcal{T} is a set of augmentation operations for generating the views. Negative views (Neg_i) are a set of graphs, which are typically randomly sampled from all graphs or from graphs whose labels differ from G_i . One typical of the contrastive loss $\mathcal{L}_{cl}(f_\theta, \hat{G}_i, \tilde{G}_i, Neg_i)$ in Equation (13) can be defined based on InfoNCE loss [105, 119] as follows:

$$\mathcal{L}_{cl}(\cdot) = -\log \frac{s(\hat{\mathbf{h}}_i, \tilde{\mathbf{h}}_i)}{\sum_{G'_i \in \{\hat{G}_i, \tilde{G}_i\}} \sum_{G_j \in A(G_i)} s(\hat{\mathbf{h}}'_i, \tilde{\mathbf{h}}_j)}, \quad (15)$$

where $A(G_i) = \hat{G}_i \cup \tilde{G}_i \cup Neg_i$ includes positive views and negative samples of G_i , and $\hat{\mathbf{h}}_i$ and $\tilde{\mathbf{h}}_i$ are the representations of graph \hat{G}_i and \tilde{G}_i , respectively. Also, $s(\mathbf{h}_i, \mathbf{h}_j) = \exp(\cosine(\mathbf{h}_i, \mathbf{h}_j)/\tau)$ is the similarity score between \mathbf{h}_i and \mathbf{h}_j based the parameter τ .

The techniques in Equation (14) are employed to generate positive views for each node. Specifically, similarity-based methods [50, 77, 92] utilize both node features and graph structures to identify nodes in the original graph, which are similar to a given target node, as the positive nodes. Also, diffusion-based approaches [36, 84, 108] modify the graph’s structure (e.g., by deleting or adding edges) based on global topological information, such as personalized PageRank (PPR) [37] and motif-preserving [84]. Perturbation-based methods [53, 86, 119, 120], on the other hand, introduce changes to both the graph’s structure and node features.

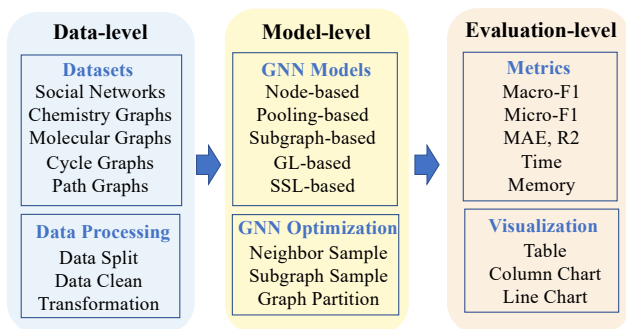


Figure 2: Evaluation framework.

4 Experiments

4.1 Evaluation Framework OpenGLT

As shown in Figure 2, we design a flexible and end-to-end evaluation framework OpenGLT that consists of three key components: the data-level, model-level, and evaluation-level components. It ensures fair and comprehensive comparisons across different methods.

- **Data-level Component.** We collected 13 datasets for graph classification spanning diverse domains, including social networks, chemical graphs, and molecular graphs, as well as 13 datasets for graph regression like cycle and path counting. Additionally, we provide a unified data processing pipeline, which includes data transformation and standardized data splits tailored to various scenarios, such as imbalanced and few-shot settings. All datasets are formatted into a unified loader to facilitate fair comparisons across different methods and support future extensions.
- **Model-level Component.** At the model level, we provide more than 20 GNN models to support comprehensive evaluations. These include node-based models, pooling-based models, subgraph-based models, graph-level models (GL-based), and self-supervised learning-based models (SSL-based). Additionally, we incorporate various optimization strategies tailored to GNNs, such as neighbor sampling, subgraph sampling, and graph partitioning, to enhance scalability and performance.
- **Evaluation-level Component.** It focuses on ensuring fair and comprehensive comparisons of model performance. We utilize a wide range of metrics, including Macro-F1, Micro-F1, Mean Absolute Error (MAE), and R^2 scores, as well as resource-based measures such as runtime and memory consumption. To aid in the interpretation of results, we provide multiple visualization options, including tables, column charts, and line charts, enabling clear and insightful comparisons across different methods.

Our framework is designed to be user-friendly and highly extensible. Users can easily integrate new GNN models by following a standardized interface and registering them in the model library. Similarly, new datasets can be incorporated by formatting them into our unified loader, which handles preprocessing and splits automatically. The evaluation module also supports the addition of custom metrics and visualizations. To assist users, we provide comprehensive documentation with examples, ensuring that the framework can be readily extended to meet diverse research needs.

4.2 Datasets

We evaluate GNNs on four domains with 26 datasets: social networks (SN), biology (BIO), chemistry (CHE), and motif counting (MC). For dataset splitting, if a standard split is publicly available and commonly used in existing works, we adopt the standard split. If there is no standard split, we use a 10-fold cross-validation approach. Detailed statistics and description are in Table 3.

4.2.1 Social Networks.

- **IMDB-BINARY (I-B)** [71] and **IMDB-MULTI (I-M)** [71]. Two movie datasets from IMDB [43] where each graph represents a movie, with nodes as actors and edges indicating co-appearance. The task of IMDB-B is to classify movies into two genres: Action and Romance. IMDB-M extends this to a three-class setting: Comedy, Action, and Drama.
- **REDDIT (RED)** [71]. We use the binary version (REDDIT-BINARY) of a dataset from Reddit [79], where each graph represents a discussion thread. Nodes correspond to users, and edges indicate interactions. The task is to classify threads into two categories: Q&A-based and Discussion-based.
- **COLLAB (COL)** [71]. A scientific collaboration dataset where each graph represents an ego-network of a researcher, with nodes as researchers and edges indicating co-authorship. The task is to classify the networks into one of three research fields: High Energy Physics, Condensed Matter Physics, or Astrophysics.

4.2.2 Biology.

- **PROTEINS (PRO)** [71] and **DD** [71]. Two binary classification datasets where each graph represents a protein. The task is to classify a protein molecule as either an enzyme or a non-enzyme. In PROTEINS, nodes represent secondary structure elements (SSEs), while in DD, nodes are amino acids; edges in both indicate spatial proximity.
- **ENZYMES (ENZ)** [71]. A six-class classification dataset from the BRENDA enzyme database. Each graph represents a protein, in which nodes represent SSEs with features encoding atomic properties, and edges denote spatial proximity. The task is to classify proteins into one of six enzyme commission (EC) classes.
- **MolHIV (HIV)** [39] and **MolTox21 (TOX)** [39]. Two molecular property prediction datasets where nodes represent atoms and edges denote chemical bonds. MolHIV is a single-label binary dataset and the task is to predict whether a molecule inhibits HIV replication. MolTox21 is a 12-label binary dataset, each label represents a specific toxicological target.

4.2.3 Chemistry. MUTAG, NCI1, MolBACE, and MolPCBA are molecular graph datasets, where nodes represent atoms and edges represent chemical bonds.

- **MUTAG (MUT)** [71] and **NCI1 (NCI)** [71]. In both datasets, node features are one-hot encodings of atomic species (e.g., C, N, O). They are binary classification tasks: MUTAG labels indicate whether a molecule is mutagenic, while NCI1 labels indicate anti-cancer activity in cell-based assays.
- **MolBACE (BAC)** [39] and **MolPCBA (PCB)** [39]. In both datasets, node features are derived from RDKit, including properties such as chirality and aromaticity. MolBACE is a single-label binary task for predicting whether a molecule inhibits the

Table 3: Data statistics. Nodes and Edges denote the average number of nodes and edges per graph, respectively. Split is the data partition strategy, where 10-fold denotes 10-fold cross-validation, others denote train/validation/test splits.

Type	Dataset	Graphs	Nodes	Edges	Classes	Split
SN	IMDB-B (I-B)	1,000	19.8	96.5	2	10-fold
	IMDB-M (I-M)	1,500	13.0	65.9	3	10-fold
	REDDIT-B (RED)	2,000	429.6	497.8	2	10-fold
	COLLAB (COL)	5,000	74.5	2457.8	3	10-fold
BIO	PROTEINS (PRO)	1,113	39.1	72.8	2	10-fold
	DD	1,178	284.3	715.7	2	10-fold
	ENZYMES (ENZ)	600	32.6	62.1	6	10-fold
	MolHIV (HIV)	41,127	25.5	54.9	2	8/1/1
	MolTox21 (TOX)	7,831	18.9	39.2	12	8/1/1
CHE	MUTAG (MUT)	188	17.9	19.8	2	10-fold
	NC11 (NCI)	4,110	29.9	32.3	2	10-fold
	MolBACE (BAC)	1,513	34.1	36.9	2	8/1/1
	MolPCBA (PCB)	437,929	26.0	28.1	128	8/1/1
MC	{3,4,5,6,7,8}-Cycle	5,000	18.8	31.3	1	3/2/5
	{4,5,6}-Path	5,000	18.8	31.3	1	3/2/5
	4-Clique	5,000	18.8	31.3	1	3/2/5
	Tailed Tri.	5,000	18.8	31.3	1	3/2/5
	Chor. Cyc.	5,000	18.8	31.3	1	3/2/5
	Tri. Rec.	5,000	18.8	31.3	1	3/2/5

BACE-1 enzyme (linked to Alzheimer’s disease). MolPCBA is a 128-label binary task, each representing activity in a specific biological assay.

4.2.4 Motif-Counting Graphs. The graphs and their splits are sourced from [10] and have been widely used in follow-up works [10, 42, 102, 114]. Each graph is labeled with the counts of specific substructures, including Cycles (3-8 nodes), Paths (4-6 nodes), 4-Cliques, Tailed Triangles, Chordal Cycles, and Triangle-Rectangles. Graphs are generated by sampling a d -regular graph with m nodes and randomly deleting m edges, where (m, d) is uniformly chosen from $\{(10, 6), (15, 6), (20, 5), (30, 5)\}$. The ground-truth counts are computed using the subgraph counting algorithm proposed in [82].

4.3 Evaluated GNNs

We comprehensively evaluate 16 representative and effective GNNs across five categories as follows.

4.3.1 Node-based GNNs.

- **GCN [48].** As a foundational GNN, GCN learns node features by aggregating information from their neighborhood, effectively performing a weighted average of neighbor representations in each layer.
- **GIN [101].** GIN utilizes a Multi-Layer Perceptron (MLP) to update node representations based on a sum of its neighbors, theoretically matching the capability of the Weisfeiler-Lehman (1-WL) graph isomorphism test.
- **GraphSAGE (SAGE) [35].** SAGE introduces a sampling-based neighborhood aggregation strategy. For each node, it uniformly samples a fixed number of neighbors to generate embeddings, making the learning process scalable and inductive.
- **PNA [12].** PNA combines multiple aggregators (e.g., mean, max, sum) with degree-based scalars to capture the distribution of

neighbor features, allowing the model to distinguish diverse neighbor patterns better than single-aggregator methods.

4.3.2 Pooling-based GNNs.

- **TopK [8, 30].** TopK uses a trainable projection vector to score nodes, with the top-k nodes passing GNN backbones selected to form the graph for the subsequent layer.
- **GMT [3].** GMT introduces a hierarchical pooling method where nodes are adaptively grouped into clusters using a transformer-based attention mechanism, allowing the model to learn soft cluster assignments and generate coarse-grained graph representations at multiple scales.
- **EdgePool (EPool) [17].** EPool learns a hierarchical representation by iteratively contracting edges. It scores edges based on their importance for connecting nodes and merges the corresponding node pairs, effectively simplifying the graph topology layer by layer.

4.3.3 Subgraph-based GNNs.

- **ECS [102].** ECS boosts the GNN backbones by injecting pre-calculated structural information. It computes embeddings that encode subgraph-centric distances, allowing the model to count substructures with provable guarantees.
- **GNNAK+ (AK+) [115].** AK+ shifts the computational unit from single-node neighborhoods to k-hop subgraphs, thereby enabling the GNN backbones to capture more complex, high-order structural patterns.
- **I2GNN (I2) [42].** I2GNN breaks structural symmetries by assigning unique identifiers to the central root node and its neighbors within each sampled subgraph, enabling finer-grained representation learning.

4.3.4 GL-based GNNs.

- **VIBGSL (VIB) [85].** VIB uses the Information Bottleneck principle to mask irrelevant features and learn a task-relevant graph structure for better modeling the key patterns.
- **HGP-SL (HGP) [112].** HGP selects key nodes to form an induced subgraph and refines the graph structure using sparse attention-based structure learning.
- **MOSGSL (MO) [118].** MO reconstructs key subgraphs using a motif-driven guidance module that dynamically captures and aligns discriminative structural patterns.

4.3.5 SSL-based GNNs.

- **RGC [84].** RGC employs a diverse-curvature GCN and motif-aware contrastive learning on a stable kernel layer to robustly model motif regularity and learn node representations.
- **MVGRL (MVG) [36].** MVG learns graph representations by contrasting node embeddings from the original and diffusion-based views of the graph.
- **GCA [119].** GCA learns graph representations by contrasting node embeddings across adaptively augmented views that preserve important structural and semantic information.

4.4 Evaluation Metric

We evaluate the performance of GNNs using effectiveness and efficiency metrics as follows.

4.4.1 Effectiveness Metric. Given a graph set $\mathcal{LG} = \{(G_i, y_i)\}_{i=1}^{|\mathcal{LG}|}$, we denote the prediction label of each graph G_i as \hat{y}_i . For graph classification tasks, we use the **Strict Accuracy (Acc)**, **Micro-F1 (Mi-F1)**, and **Macro-F1 (Ma-F1)**. Particularly, if each graph only has one label, the **Micro-F1** is same as **Accuracy**.

- **Strict Accuracy (Acc).** Strict accuracy is used to measure the proportion of exact matches between predicted and true labels. Strict accuracy is defined as $Acc = \frac{1}{|\mathcal{LG}|} \sum_{G_i \in \mathcal{LG}} \mathbb{I}(y_i = \hat{y}_i)$, where $\mathbb{I}(y_i = \hat{y}_i) = 1$ if only $y_i = \hat{y}_i$.
- **Micro-F1 (Mi-F1).** Micro-F1 is a performance metric that considers the overall precision and recall across all instances in the dataset. The Micro-precision is defined as $Mi-P = \frac{\sum_{G_i \in \mathcal{LG}} |y_i \cap \hat{y}_i|}{\sum_{G_j \in \mathcal{LG}} |\hat{y}_j|}$ and Micro-recall is $Mi-R = \frac{\sum_{G_i \in \mathcal{LG}} |y_i \cap \hat{y}_i|}{\sum_{G_j \in \mathcal{LG}} |y_j|}$. Then, the Micro-F1 is defined as $Mi-F1 = \frac{2 \times Mi-P \times Mi-R}{Mi-P + Mi-R}$.
- **Macro-F1 (Ma-F1).** Macro-F1 evaluates the average performance of precision and recall across all instances, treating each equally regardless of size. The Macro-precision is defined as $Ma-P = \frac{1}{|\mathcal{LG}|} \sum_{G_i \in \mathcal{LG}} \frac{|y_i \cap \hat{y}_i|}{|\hat{y}_i|}$ and Macro-recall is defined as $Ma-R = \frac{1}{|\mathcal{LG}|} \sum_{G_i \in \mathcal{LG}} \frac{|y_i \cap \hat{y}_i|}{|y_i|}$, so the Macro-F1 is defined as $Ma-F1 = \frac{2 \times Ma-P \times Ma-R}{Ma-P + Ma-R}$.

For graph regression tasks, we use the **Mean Absolute Error (MAE)** and **R2** as follows.

- **Mean Absolute Error (MAE).** Mean Absolute Error measures the average magnitude of errors between predicted and true values. MAE is defined as $MAE = \frac{1}{|\mathcal{LG}|} \sum_{G_i \in \mathcal{LG}} |y_i - \hat{y}_i|$. Lower MAE indicates better performance.
- **R2.** R2 evaluates the proportion of variance in the true values that is captured by the predicted values. The R2 is defined as $R2 = 1 - \frac{\sum_{G_i \in \mathcal{LG}} (y_i - \hat{y}_i)^2}{\sum_{G_i \in \mathcal{LG}} (y_i - \bar{y})^2} \in [0, 1]$, where $\bar{y} = \frac{1}{|\mathcal{LG}|} \sum_{G_i \in \mathcal{LG}} y_i$ is the mean of the true values. Higher R2 indicates better performance.

4.4.2 Efficiency Metric. We evaluate the efficiency of models on both graph classification and regression tasks based on the **training time (s)**, **inference time (s)**, **memory usage (MB)** in training and inference phases.

4.5 Hyperparameter and Hardware Setting

For classification datasets, we set the batch size as 32 for four larger datasets (REDDIT, COLLAB, DD, and MolPCBA) and 128 for the other datasets. For regression datasets, we set the batch size as 256. To efficiently tune the hyperparameters for each model, we employed the Optuna framework [2]. For each model, we conducted 200 trials using the Tree-structured Parzen Estimator (TPE) sampler and a MedianPruner to terminate unpromising trials early. The hyperparameter search spaces were defined as follows: the hidden dimension is selected from {64, 128, 256, 512}, the learning rate from $\{1e-2, 1e-3, 1e-4, 1e-5\}$, GNN layers from {1, 2, 3, 4}, and the dropout rate from {0, 0.1, 0.2, 0.3, 0.4, 0.5}. All models are trained for a maximum of 2000 epochs, with early stopping applied if no improvement is observed on the validation set within 50 epochs.

All experiments are executed on a CentOS 7 machine equipped with dual 10-core Intel® Xeon® Silver 4210 CPUs @ 2.20GHz, 8 NVIDIA GeForce RTX 2080 Ti GPUs (11GB each) and 256GB RAM.

4.6 Effectiveness Evaluation

4.6.1 Graph Classification Tasks. As shown in Table 4, node-based GNNs, such as GCN and SAGE, cannot achieve satisfactory performance. These models learn node representations and use global pooling. Global pooling overlooks local structural information, which is critical for distinguishing graphs in bioinformatics (e.g., ENZYMES) and chemistry (e.g., MUTAG). PNA achieves comparatively good performance as it captures richer neighborhood distributions by leveraging multiple aggregators and degree-scalers. Secondly, pooling-based approaches, such as GMT and TopK, achieve competitive performance, particularly on social networks like COLLAB and REDDIT. These methods progressively reduce the graph size by grouping nodes or retaining only the most important ones, thereby preserving multi-level structural information. However, they are less effective on datasets where fine-grained local structures (e.g., motifs) play a critical role, such as ENZYMES and NCI1. Subgraph-based methods, such as ECS, AK+, and I2, demonstrate highly competitive performance on bioinformatics and chemistry datasets because they break graphs into meaningful substructures, enabling them to capture important patterns that other methods often miss. However, they are out-of-memory (OOM) on large graphs or high node counts, such as REDDIT and COLLAB. Fourthly, graph learning-based approaches, such as MO and HGP, perform well on noisy social datasets, such as IMDB-B and IMDB-M. By dynamically reconstructing graph structures and removing irrelevant edges or nodes, these approaches enhance robustness and improve generalization. However, they are less effective on datasets where the original graph structure is already well-formed molecular graphs, such as MUTAG. Lastly, SSL-based methods like MVG and GCA perform robustly across multiple datasets, leveraging pretraining on unlabeled graphs to learn generalizable representations. However, SSL-based approaches are computationally expensive due to graph augmentation and can lead to OOM issues.

4.6.2 Graph Regression Tasks. For graph regression tasks, the focus is primarily on evaluating how well GNNs can capture the semantics and key structural patterns of graphs, such as cycle and path counts for each graph. Lower MAE and higher R^2 scores reflect better performance. As shown in Table 5, node-based methods (excluding GIN and PNA), pooling-based models, GL-based techniques, and SSL-based approaches generally fail to deliver satisfactory results. This is because these methods are not specifically designed to enhance the expressiveness of GNNs, meaning they cannot effectively differentiate between isomorphic graphs or graphs with identical cycles. In contrast, GIN, PNA, and subgraph-based GNNs explicitly aim to improve the theoretical expressiveness of GNNs, resulting in superior performance. GIN and PNA aim to improve the theoretical expressiveness to approximate the Weisfeiler-Lehman (1-WL) isomorphism test. Subgraph-based models like ECS, AK+, and I2 consistently outperform other approaches on almost all regression datasets. By breaking graphs down into overlapping or rooted subgraphs, these methods capture rich structural details that enhance their theoretical expressivity. As a result, they are better able to distinguish between graph isomorphism classes and accurately identify important motifs, which leads to improved performance. Lastly, as the complexity of the target motif increases (e.g., from 3-Cycle to 8-Cycle), most GNNs (except subgraph-based

Table 4: Evaluation on graph classification. The best and second performance are highlighted in bold and underlined, respectively. “Met.” means Metrics, “OOM” means out-of-memory, and “> 3days” means training cannot be completed within 3 days.

Type	Data	Met.	Node-based				Pooling-based			Subgraph-based			GL-based			SSL-based		
			GCN	GIN	SAGE	PNA	TopK	GMT	EPool	ECS	AK+	I2	VIB	HGP	MO	RGC	MVG	GCA
SN	I-B	Acc	0.6840	0.7100	0.6860	0.7280	0.6860	0.7440	0.6980	0.7150	0.7290	0.7070	0.7250	0.7030	<u>0.7310</u>	0.6230	0.6970	0.7120
		F1	0.6963	0.7117	0.6991	0.7391	0.7105	0.7625	0.7146	0.7158	0.7391	0.7014	0.7185	0.7078	<u>0.7422</u>	0.6321	0.6940	0.7147
	I-M	Acc	0.4620	0.4820	0.4650	0.4980	0.4670	0.5080	0.4750	0.4727	0.4967	OOM	0.4720	0.4650	<u>0.5067</u>	0.4130	0.4867	0.4833
		F1	0.4393	0.4706	0.4512	0.4842	0.4435	<u>0.4850</u>	0.4563	0.4466	0.4839	OOM	0.4443	0.4376	0.4874	0.3867	0.4788	0.4726
	RED	Acc	0.9029	0.8965	0.9094	OOM	0.9280	0.9195	<u>0.9260</u>	OOM	OOM	OOM	0.8276	OOM	0.8625	OOM	OOM	OOM
		F1	0.9123	0.9026	0.9132	OOM	0.9322	0.9263	<u>0.9303</u>	OOM	OOM	OOM	0.8298	OOM	0.8722	OOM	OOM	OOM
	COL	Acc	0.7644	0.7328	0.7406	OOM	0.7556	<u>0.8164</u>	0.7696	OOM	OOM	OOM	0.7528	0.6988	0.8278	OOM	0.7688	OOM
		F1	0.7454	0.7099	0.7169	OOM	0.7395	<u>0.7973</u>	0.7520	OOM	OOM	OOM	0.7114	0.6702	0.8046	OOM	0.7320	OOM
BIO	PRO	Acc	0.7286	0.7250	0.7367	0.7372	0.7277	<u>0.7440</u>	0.7286	0.7061	0.7475	0.7071	0.7322	0.7304	0.7232	0.7015	0.7367	0.7322
		F1	0.6596	0.6432	0.6617	0.6645	0.6712	0.7058	0.6598	0.5838	0.6978	0.6026	0.6641	0.6653	0.6442	0.6386	<u>0.6993</u>	0.6647
	DD	Acc	0.7310	0.7233	0.7542	0.7488	0.7156	0.7802	0.7343	OOM	<u>0.7776</u>	0.7335	0.7632	0.7598	0.7632	OOM	OOM	OOM
		F1	0.6676	0.6555	0.6707	0.7245	0.6384	<u>0.7252</u>	0.6687	OOM	0.7267	0.6402	0.6845	0.6841	0.6844	OOM	OOM	OOM
	ENZ	Acc	0.4650	0.4833	0.5183	0.5233	0.4800	0.4950	0.4783	0.4617	<u>0.5267</u>	0.4650	0.4417	0.4667	0.5250	0.4917	0.5317	0.4817
		F1	0.4775	0.4781	0.5098	0.5204	0.4794	0.4237	0.4737	0.4592	<u>0.5279</u>	0.4628	0.4337	0.4695	<u>0.5309</u>	0.4902	0.5314	0.4772
	HIV	Acc	0.9696	0.9701	0.9695	0.9703	0.9687	0.9691	0.9696	0.9689	0.9728	0.9703	0.9686	0.9689	0.9701	0.9686	<u>0.9705</u>	0.9701
		F1	0.3192	0.3466	0.2991	0.3622	0.2221	0.2861	0.3213	0.2537	0.3682	0.3413	0.2203	0.2518	0.2502	0.2225	<u>0.3628</u>	0.3448
	TOX	Acc	0.5548	0.5553	0.5529	0.5561	0.5523	0.5412	0.5514	0.5463	0.5561	0.5580	0.5283	0.5350	0.5384	0.5112	<u>0.5565</u>	0.5558
		F1-i	0.9120	0.9114	0.9096	0.9135	0.9083	0.9109	0.9101	0.9121	0.9138	<u>0.9137</u>	0.8993	0.9004	0.9048	0.8986	0.9126	0.9123
	F1-a	0.3628	0.3601	0.3418	0.3839	0.2240	0.3452	0.3765	0.3858	<u>0.3850</u>	0.3815	0.2020	0.2125	0.2180	0.1981	0.3847	0.3695	
CHE	MUT	Acc	0.8041	0.8570	0.8199	0.8588	0.8094	0.8254	0.8091	0.8091	0.8409	0.8062	0.7643	0.7706	0.7790	0.7067	0.8607	0.8842
		F1	0.8583	0.8907	0.8644	0.8909	0.8590	0.8642	0.8506	0.8558	0.8770	0.8512	0.8255	0.8296	0.8447	0.8012	<u>0.8912</u>	0.9070
	NCI	Acc	0.8158	0.8154	0.8146	<u>0.8183</u>	0.8169	0.7662	0.8160	0.7866	0.8187	0.7603	0.7816	0.7825	0.7852	0.6995	0.7560	0.8122
		F1	0.8160	0.8153	0.8149	<u>0.8184</u>	0.8171	0.7708	0.8168	0.7914	0.8190	0.7673	0.7827	0.7831	0.7855	0.6997	0.7557	0.8119
	BAC	Acc	0.6711	0.6645	0.6477	0.7074	0.6756	0.6513	0.6749	0.7125	0.6803	0.6078	0.6019	0.6689	0.6294	0.6089	<u>0.7099</u>	0.6729
		F1	0.7154	0.7351	0.7099	0.7342	0.7264	0.7366	0.7436	<u>0.7400</u>	0.7382	0.7055	0.7001	0.6545	0.7077	0.7047	0.7366	0.7186
	PCB	Acc	0.5456	0.5466	0.5451	<u>0.5470</u>	0.5461	0.5447	> 3days	OOM	0.5523	0.5414	OOM	OOM	OOM	OOM	OOM	OOM
		Mi-F1	0.9850	<u>0.9853</u>	0.9839	<u>0.9853</u>	0.9849	0.9836	> 3days	OOM	0.9860	0.9850	OOM	OOM	OOM	OOM	OOM	OOM
	Ma-F1	0.1200	0.1500	0.1317	0.1517	0.1333	0.0167	> 3days	OOM	0.2140	<u>0.2064</u>	OOM	OOM	OOM	OOM	OOM	OOM	

ones) experience a drastic performance drop. This highlights the limitations of many GNN architectures in capturing higher-order dependencies and complex structural relationships.

4.7 Efficiency Evaluation

We evaluate the efficiency of GNNs in terms of total training time, inference time, GPU peak memory usage during training and inference. As shown in Table 6, node-based GNNs exhibit the highest efficiency across all datasets. Their simplicity in aggregating neighbors’ information without additional graph processing ensures minimal time and memory usage. However, this efficiency comes at the cost of limited expressiveness as discussed in Section 4.6. Secondly, pooling-based methods strike a balance between efficiency and performance. TopK is efficient due to its node-pruning strategy, which reduces graph size while preserving key features. However, more advanced pooling approaches, such as GMT, are computationally expensive due to their clustering operations based on node similarity. Thirdly, subgraph-based GNNs (e.g., ECS, AK+, I2) are computationally intensive because they rely on generating multiple subgraphs for each graph. Despite their high resource requirements,

these methods excel at capturing graph motifs and complex structural patterns, as shown in Section 4.6. Their computational cost makes them less efficient for real-time or large-scale applications. GL-based methods (e.g., VIB, HGP, and MO) dynamically reconstruct graph structures during training, which adds significant computational overhead. While they improve robustness to noise and graph quality, their iterative optimization process limits scalability to larger datasets. SSL-based methods (e.g., RGC, MVG, GCA) are computationally expensive during training because they require graph augmentations and additional contrastive learning stage.

In summary, node-based GNNs are the most efficient but lack expressiveness, while pooling-based models strike a balance between efficiency and performance. Subgraph-based and GL-based approaches offer superior expressiveness but suffer from high computational costs. SSL-based methods, though computationally expensive during training, are efficient during inference, making them suitable for pretraining scenarios.

4.8 More Scenarios

We further evaluate GNNs in three realistic and challenging scenarios, including noisy graphs, imbalanced graphs, and few-shot

Table 5: Evaluation on graph regression. The best and second performance are highlighted in bold and underlined, respectively.

Type	Data	Met.	Node-based				Pooling-based			Subgraph-based			GL-based			SSL-based		
			GCN	GIN	SAGE	PNA	TopK	GMT	EPool	ECS	AK+	I2	VIB	HGP	MO	RGC	MVG	GCA
MC	3-Cyc	MAE	0.4396	0.3962	0.5119	0.4060	0.4290	0.4251	0.4238	0.0192	<u>0.0022</u>	0.0009	0.8776	0.4369	0.5410	0.4744	0.4231	0.3873
		R2	0.6970	0.7546	0.8081	0.7493	0.7044	0.7107	0.5679	0.9996	<u>0.9998</u>	0.9999	0.1025	0.6850	0.5003	0.6062	0.7174	0.7595
	4-Cyc	MAE	0.2806	0.2536	0.5407	0.2509	0.2772	0.2720	0.2696	<u>0.0148</u>	0.0223	0.0062	0.6451	0.2745	0.5442	0.5398	0.2734	0.2204
		R2	0.8229	0.8864	0.4011	0.8924	0.8331	0.8477	0.8406	<u>0.9997</u>	0.9990	0.9998	0.1424	0.8350	0.4032	0.4436	0.8606	0.8987
	5-Cyc	MAE	0.2782	0.1858	0.4608	0.2580	0.2399	0.2338	0.2659	0.0716	<u>0.0340</u>	0.0115	0.9021	0.2763	0.4532	0.4570	0.2180	0.1756
		R2	0.8334	0.9364	0.4815	0.8866	0.8614	0.8936	0.8553	0.9862	<u>0.9972</u>	0.9996	0.0019	0.8190	0.6081	0.4939	0.9060	0.9408
	6-Cyc	MAE	0.3014	0.1895	0.4690	0.2841	0.2302	0.1788	0.2926	0.0862	<u>0.0584</u>	0.0368	0.8876	0.3035	0.4557	0.5027	0.1773	0.1784
		R2	0.7926	0.9162	0.6189	0.8252	0.8803	0.9279	0.8073	0.9569	<u>0.9956</u>	0.9969	0.0021	0.7891	0.6219	0.6077	0.9301	0.9223
	7-Cyc	MAE	0.4011	0.2111	0.5898	0.2237	0.2852	0.1569	0.3942	0.1560	<u>0.0563</u>	0.0488	0.8273	0.4220	0.5713	0.5836	0.1500	0.2045
		R2	0.5887	0.8635	0.4594	0.8469	0.7921	0.9354	0.6091	0.9460	<u>0.9937</u>	0.9946	0.0064	0.5487	0.4883	0.4692	0.9404	0.8770
	8-Cyc	MAE	0.4757	0.2632	0.5285	0.2841	0.2910	0.1377	0.4701	0.1153	<u>0.0493</u>	0.0399	0.7430	0.4790	0.5340	0.4808	0.1286	0.2592
		R2	0.3570	0.7220	0.2212	0.7152	0.7553	0.9428	0.3840	0.9703	<u>0.9949</u>	0.9963	0.0330	0.3520	0.2051	0.3319	0.9466	0.7265
	4-Path	MAE	0.7154	0.4273	0.7340	0.2940	0.5273	0.1606	0.6361	0.0243	<u>0.0150</u>	0.0083	0.7784	0.5019	0.7316	0.7270	0.1512	0.4093
		R2	0.1574	0.6349	0.0898	0.8619	0.5270	0.9459	0.3188	0.9921	<u>0.9996</u>	0.9998	0.0279	0.5390	0.0909	0.1310	0.9534	0.6579
	5-Path	MAE	0.6848	0.3949	0.6669	0.3628	0.5189	0.1559	0.6133	<u>0.0134</u>	0.0153	0.0092	0.7510	0.4846	0.6933	0.7053	0.1407	0.3805
		R2	0.1050	0.6358	0.1675	0.6973	0.5015	0.9473	0.3254	<u>0.9995</u>	<u>0.9995</u>	0.9998	0.0283	0.5204	0.0823	0.0650	0.9562	0.6562
	6-Path	MAE	0.6164	0.3913	0.6594	0.3397	0.5629	0.1394	0.6930	0.0138	<u>0.0133</u>	0.0089	0.7571	0.4552	0.6627	0.6589	0.1299	0.3784
		R2	0.2470	0.5958	0.1286	0.7429	0.4133	0.9539	0.1408	0.9995	<u>0.9996</u>	0.9998	0.0250	0.5459	0.1282	0.1280	0.9607	0.6076
4-Cliq	MAE	0.3432	0.3449	0.3498	0.2504	0.3430	0.3427	0.3578	<u>0.0090</u>	0.0092	0.0005	0.3866	0.2355	0.3422	0.3424	0.1797	0.3401	
	R2	0.1612	0.1348	0.1086	0.8230	0.1213	0.1022	0.1057	<u>0.9665</u>	<u>0.9964</u>	0.9999	0.0890	0.8896	0.1604	0.1610	0.9002	0.1644	
Tailed Tri	MAE	0.3506	0.2886	0.3812	0.3470	0.3465	0.3665	0.3405	0.0189	<u>0.0146</u>	0.0034	0.8934	0.3791	0.3891	0.4095	0.3277	0.2747	
	R2	0.7884	0.8606	0.7303	0.7792	0.7813	0.7673	0.8053	0.9989	<u>0.9995</u>	0.9999	0.0176	0.7336	0.7008	0.6245	0.8177	0.8662	
Chor. Cyc	MAE	0.4377	0.3683	0.4390	0.3500	0.4216	0.3690	0.4246	<u>0.0295</u>	0.0336	0.0044	0.8720	0.4441	0.4413	0.4728	0.3671	0.3608	
	R2	0.6346	0.7109	0.6002	0.8121	0.6414	0.6848	0.6421	<u>0.9970</u>	0.9951	0.9999	0.0333	0.5746	0.5841	0.5684	0.7293	0.7149	
Tri. Rec.	MAE	0.4657	0.4034	0.4794	0.4410	0.4736	0.4068	0.4890	0.3619	<u>0.3464</u>	0.3271	0.8263	0.4286	0.4755	0.5409	0.4301	0.3943	
	R2	0.5211	0.6291	0.5335	0.5598	0.4921	0.6235	0.4702	0.6895	<u>0.7063</u>	0.7241	0.0338	0.5828	0.5037	0.3852	0.5691	0.6425	

Table 6: Efficiency evaluation. We report total training (Train (s)) and inference (Infer (s)) times with two decimal places, and GPU memory usage for training (T-Mem (MB)) and inference (I-Mem (MB)) in integers. "OOM" indicates out-of-memory.

Type	Data	Met.	Node-based				Pooling-based			Subgraph-based			GL-based			SSL-based		
			GCN	GIN	SAGE	PNA	TopK	GMT	EPool	ECS	AK+	I2	VIB	HGP	MO	RGC	MVG	GCA
SN	RED	Train(s)	192.44	<u>182.98</u>	179.55	OOM	218.03	758.22	8365.60	OOM	OOM	OOM	OOM	OOM	371.86	OOM	OOM	OOM
		Infer(s)	28.42	<u>26.21</u>	26.04	OOM	32.95	30.45	1953.91	OOM	OOM	OOM	OOM	OOM	79.35	OOM	OOM	OOM
		T-Mem(MB)	287	<u>288</u>	310	OOM	287	2120	360	OOM	OOM	OOM	OOM	OOM	604	OOM	OOM	OOM
		I-Mem(MB)	190	122	<u>135</u>	OOM	190	244	194	OOM	OOM	OOM	OOM	OOM	289	OOM	OOM	OOM
BIO	ENZ	Train(s)	<u>26.05</u>	26.34	25.23	72.33	31.95	38.85	375.25	312.46	350.25	470.05	120.48	67.50	75.29	495.23	57.53	125.45
		Infer(s)	5.19	5.33	5.04	17.42	6.84	7.17	76.30	68.74	68.93	94.92	36.12	19.20	28.27	85.11	7.76	<u>5.07</u>
		T-Mem(MB)	83	<u>78</u>	77	289	83	228	103	582	2369	1656	323	186	506	282	324	272
		I-Mem(MB)	<u>42</u>	36	36	96	<u>42</u>	46	45	270	879	790	152	95	194	54	58	<u>42</u>
CHE	MUT	Train(s)	<u>10.78</u>	11.03	10.05	24.53	13.50	15.96	60.13	52.05	88.70	67.33	44.37	35.32	39.99	80.49	25.15	20.72
		Infer(s)	<u>3.86</u>	3.89	3.51	7.94	5.27	4.01	17.74	18.91	21.18	25.10	15.80	11.63	15.18	29.78	7.64	3.94
		T-Mem(MB)	42	<u>44</u>	<u>44</u>	152	42	82	46	422	775	1306	56	48	431	134	140	104
		I-Mem(MB)	19	<u>20</u>	21	82	19	24	19	245	210	722	26	27	74	24	25	19
MC	4-Cyc	Train(s)	166.50	<u>160.95</u>	140.88	458.70	180.57	1224.39	482.95	1180.51	645.97	1487.66	395.71	284.34	394.60	1770.94	300.21	304.95
		Infer(s)	256.17	<u>241.02</u>	235.40	590.20	279.43	2058.62	1033.68	1776.91	920.13	2219.63	549.60	441.95	583.55	2675.22	461.87	262.40
		T-Mem(MB)	<u>88</u>	85	85	228	<u>88</u>	380	104	1214	1734	3080	262	269	470	238	237	165
		I-Mem(MB)	<u>64</u>	62	62	209	<u>64</u>	260	68	342	608	726	104	152	270	103	96	<u>64</u>

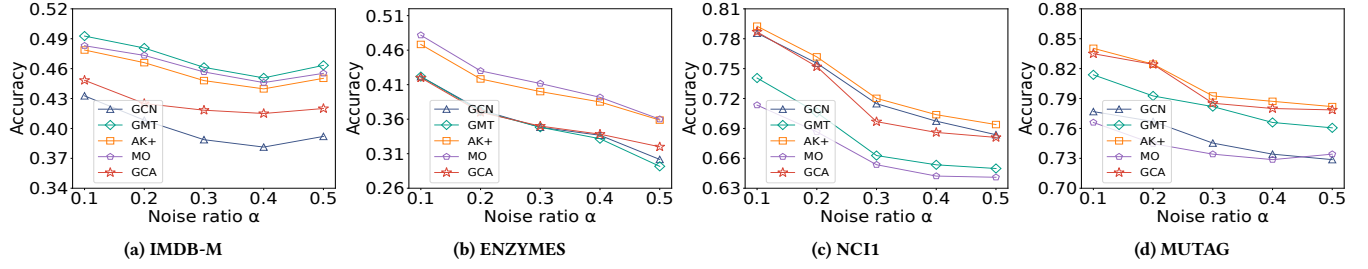


Figure 3: Robustness evaluation on noisy graphs.

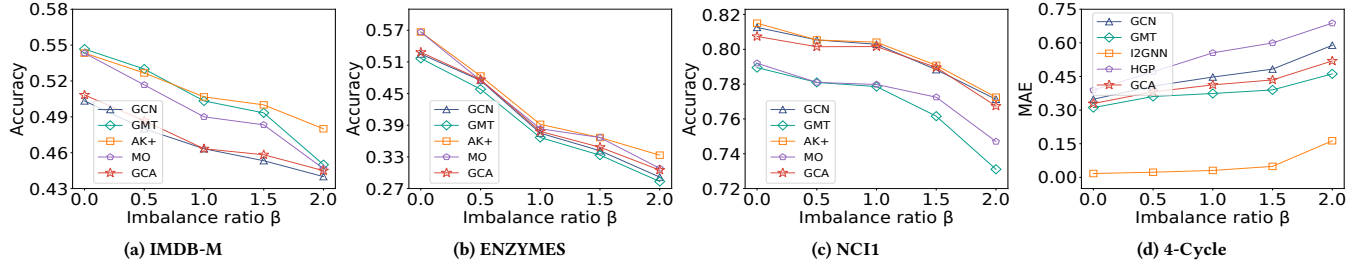


Figure 4: Imbalance data evaluation.

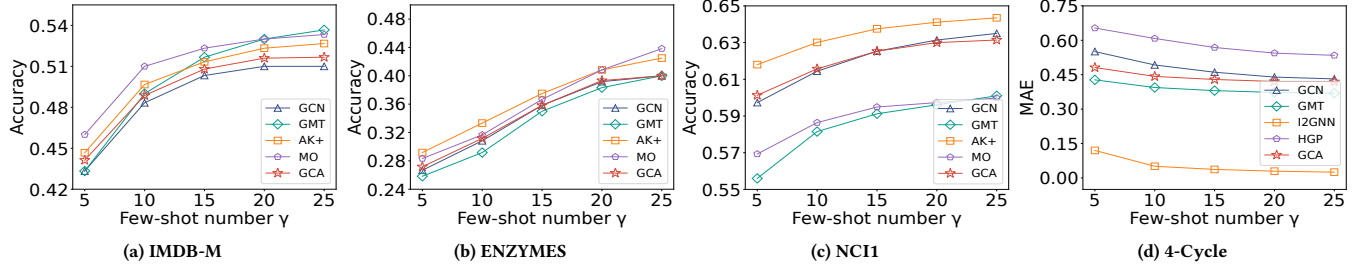


Figure 5: Few-shot evaluation.

graphs. To ensure clarity, we select one representative graph dataset from each domain for evaluation, i.e., IMDB-M, ENZYMES, NCI1, and 4-Cycle. Additionally, we compare some of the most representative models from each GNN category, including GCN (node-based), GMT (pooling-based), and GCA (SSL-based). For top perform, we select AK+ (subgraph-based), MO (GL-based) for classification tasks, while I2 (subgraph-based) and HGP (GL-based) for regression tasks.

4.8.1 Robustness Evaluation on Noisy Graphs. We assess model performance under structural noise. Specifically, for each graph $G(V, A, X)$, we introduce noise by randomly removing $\alpha|A|_0$ existing edges, where the ratio α takes values in $\{0.1, 0.2, 0.3, 0.4, 0.5\}$. As shown in Figure 3, as α increases, node-based GNNs (e.g., GCN) and Pooling-based models (e.g., GMT) suffer significant performance drops, due to their reliance on the original connectivity for aggregation and clustering. In contrast, subgraph-based methods such as AK+ show greater robustness by focusing on small, locally coherent substructures that remain intact despite global noise. Graph learning-based models like MO are even more resilient, dynamically reconstructing graph structures to mitigate the impact of noise. Similarly, SSL-based methods such as GCA perform well, leveraging

augmented views to learn noise-resistant representations. Overall, the evidence underscores that subgraph-based, GL-based, and SSL-based methods demonstrate superior robustness to noise compared to node-based and pooling-based models. This highlights the practical value of these more sophisticated methods for handling real-world graphs, which are often challenging to model due to inherent noise.

4.8.2 Imbalance Data Evaluation. For the graph classification task, given a dataset $\mathcal{G} = (G_i, y_i)$, we simulate class imbalance by adjusting the proportion of training samples in each class to follow the sequence $\{1, \frac{1}{2^\beta}, \frac{1}{3^\beta}, \dots, \frac{1}{|\mathcal{Y}|^\beta}\}$, where $\beta \in \{0, 0.5, 1, 1.5, 2\}$ determines the degree of imbalance. The sample count for the first class remains constant across all β settings. For graph regression tasks, where y_i spans the interval $[y_{\min}, y_{\max}]$, we divide the label range into three equal-sized buckets and set the group proportions as $\{1, \frac{1}{2^\beta}, \frac{1}{3^\beta}\}$ to create imbalance, with larger β corresponding to higher level of imbalance. As shown in Figure 4, accuracy drops across various GNN architectures as imbalance increases, particularly in datasets with minority classes. Node-based GNN (e.g., GCN)

and pooling-based GNN (GMT) struggle because their global aggregation mechanisms tend to average out minority signals, making it difficult to distinguish rare patterns. Subgraph-based (AK+) and graph learning-based (MO) GNNs, while capturing richer structural information, do not explicitly address class imbalance, leading to performance degradation under extreme imbalance, especially for less classes. SSL-based model (GCA), although capable of leveraging abundant unlabeled data, likewise fails to correct imbalance on its own and converges to performance similar to other baselines unless augmented with imbalance-aware strategies [66].

4.8.3 Few-shot Evaluation. We simulate data scarcity by limiting the number of training samples. For classification tasks, we construct training sets where the number of labeled graphs per class is in $\gamma \in \{5, 10, 15, 20, 25\}$. For regression tasks, we partition the label into five equal-width buckets and uniformly sample γ training instances per bucket. The results, as summarized in Figure 5, reveal that most GNN architectures exhibit significant performance degradation as γ decreases. Node-based (GCN) and pooling-based (GMT) models are particularly affected, as their global aggregation mechanisms rely heavily on abundant labeled data to learn meaningful representations. Interestingly, while subgraph-based models such as AK+ and I2, as well as graph learning-based models like MO and HGP, are theoretically capable of leveraging local structural patterns, they do not demonstrate substantial resilience to data scarcity in practice. This is primarily because current implementations lack explicit mechanisms to identify and prioritize the most informative subgraphs or adaptively focus on critical features when labeled data is limited. Their performance improvements over standard baselines are thus marginal in few-shot scenarios, indicating that richer local modeling alone does not guarantee data efficiency [96].

4.9 Correlation Analysis

4.9.1 Graph Topological Features. To investigate the intrinsic relationship between graph topology and GNN model performance, we characterize each graph using a comprehensive set of topological features. These features capture properties ranging from macroscopic global characteristics to fine-grained local patterns. We categorize them into three groups: (i) Global Structural Features, (ii) Local Structural Features, and (iii) Node Distributions.

Global Structural Features. These metrics provide a high-level summary of the entire graph’s connectivity and organization. They typically return a single scalar value for each graph.

- **Average Degree (Deg.) and Density (Den.).** For a graph $G = (V, E)$, let $|V|$ and $|E|$ be the number of nodes and edges, respectively. Avg. Deg = $\frac{2|E|}{|V|}$. Density is the ratio of actual edges to possible edges:

$$\text{Density} = \frac{2|E|}{|V|(|V| - 1)}. \quad (16)$$

They measure the overall sparsity.

- **Average Shortest Path Length (SPL) and Diameter (Dia.).** Let $d(u, v)$ denote the shortest path distance between nodes u and v . SPL = $\frac{1}{|V|(|V|-1)} \sum_{u \neq v} d(u, v)$, and Diameter = $\max_{u \neq v} d(u, v)$. For disconnected graphs, these are computed on the largest connected component.

- **Degree Assortativity (Assr.).** Calculated as the Pearson correlation coefficient between the degrees of connected nodes. Positive values indicate that high-degree nodes tend to connect with other high-degree nodes.
- **Modularity (Mod.).** Quantifies the strength of community structure. A positive value indicates that connections within communities are denser than expected by random chance.

Local Structural Features. These metrics focus on small, recurring substructures. For node-level metrics, we aggregate them into graph-level features.

- **Average Clustering Coefficient (CC).** For a node v , the local clustering coefficient C_v is the density of the subgraph induced by its neighbors. We report the average over all nodes: Avg. CC = $\frac{1}{|V|} \sum_{v \in V} C_v$.
- **Triangle Counts (Tri.).** Let T_v be the number of triangles node v participates in. Unlike global metrics, to capture both the prevalence and distribution of triangles, we report both the **mean** (μ) and **standard deviation** (σ) of T_v across all nodes. High μ implies a dense graph, while high σ indicates a significant degree of heterogeneity.

Node Distributions. These features analyze the distribution of node importance. Since these are originally defined at the node level, we characterize the entire graph by reporting both the **Mean** (μ) and **Standard Deviation** (σ) for each metric.

- **Betweenness Centrality (BC.).** $C_B(v)$ represents the fraction of all-pairs shortest paths passing through node v . We report μ_{BC} and σ_{BC} . A high σ_{BC} indicates the presence of critical "bridge" nodes controlling information flow.
- **PageRank (PR.).** Measures node influence based on transitive importance. We report μ_{PR} and σ_{PR} . A high σ_{PR} reveals a hierarchical structure with distinct authority nodes.
- **K-Core Number (KC.).** The core number k_v is the largest k such that v belongs to a k -core. We report μ_{KC} and σ_{KC} . A high μ_{KC} indicates global robustness, while high σ_{KC} reflects a core-periphery structure.

4.9.2 Evaluation. Given GNNs $\mathcal{M} = \{M_i\}_{i=1}^n$ and graph dataset $\mathcal{D} = \{G_j\}_{j=1}^m$, we construct a performance matrix $\mathbf{P} \in \mathbb{R}^{n \times m}$ where $\mathbf{P}[i][j]$ is the result of M_i on G_j (e.g., accuracy or MAE). We denote each k -th topological feature of \mathcal{D} as \mathbf{f}_k , where $\mathbf{f}_k[j]$ is the value of the k -th feature for graph G_j . We assess the relationship between model performance and k -th feature with Spearman’s correlation $\rho(\mathbf{P}[i], \mathbf{f}_k)$, with a significance threshold of $\alpha = 0.05$.

4.9.3 Insights. As illustrated in Figure 6, we observe:

- Structurally simpler models (e.g., Node-based) show weak correlations with most features, reflecting their reliance on local aggregation rather than global topology.
- Graph density negatively correlates with most models, suggesting high connectivity exacerbates over-smoothing and noise.
- High local clustering and assortativity negatively impact Subgraph-based and SSL-based models, likely due to the “rich-club” effect distracting from peripheral structures.
- Conversely, graph sparsity and high Betweenness Centrality positively correlate with Hierarchical (e.g., HGP) and SSL-based models, demonstrating their ability to leverage clear structures for long-range information flow.

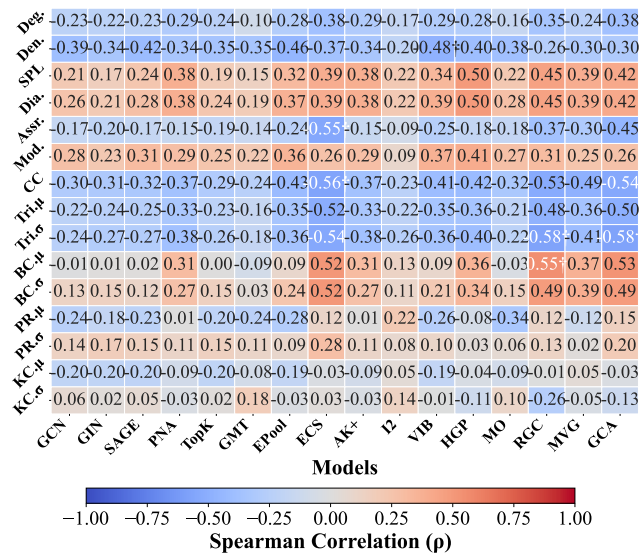


Figure 6: Correlation between graph features and GNNs. Each cell shows the Spearman’s ρ with * for $p < 0.05$ and † for $0.05 \leq p < 0.1$.

Most importantly, the absence of universally significant correlations confirms that (i) model selection cannot rely on a single structural indicator, and (ii) no single architecture consistently dominates. This underscores the critical importance of comprehensive benchmarks across diverse domains, as conducted in OPENGLT, to provide an empirical basis for scenario-specific model selection.

5 Conclusion and Future Direction

This paper presents a comprehensive experimental study on graph neural networks for graph-level tasks, categorizing existing models, introducing a unified evaluation framework (OpenGLT), and benchmarking 16 GNNs across 26 diverse datasets under challenging scenarios such as noise, imbalance, and limited data. Our results reveal that no single model excels universally, highlighting important trade-offs between expressiveness and efficiency, and emphasizing the need for robust evaluation in realistic conditions.

Based on these findings, promising future directions include the development of scenario-adaptive or hybrid GNN architectures that dynamically leverage different model strengths, research into lightweight and scalable algorithms for practical deployment, and the incorporation of transfer and foundation model techniques to improve generalization and data efficiency, particularly when labeled data is scarce. Our study provides valuable benchmarks and guidance for advancing GNN research on graph-level tasks.

References

- [1] Sami Abu-El-Haija, Bryan Perozzi, Amol Kapoor, Nazanin Alipourfard, Kristina Lerman, Hrayr Harutyunyan, Greg Ver Steeg, and Aram Galstyan. 2019. Mixhop: Higher-order graph convolutional architectures via sparsified neighborhood mixing. In *international conference on machine learning*. PMLR, 21–29.
- [2] Takuya Akiba, Shotaro Sano, Toshihiko Yanase, Takeru Ohta, and Masanori Koyama. 2019. Optuna: A Next-generation Hyperparameter Optimization Framework. *CoRR* abs/1907.10902 (2019). <http://arxiv.org/abs/1907.10902>
- [3] Jinheon Baek, Minki Kang, and Sung Ju Hwang. 2021. Accurate Learning of Graph Representations with Graph Multiset Pooling. In *9th International Conference on Learning Representations, ICLR 2021, Virtual Event, Austria, May 3–7, 2021*. OpenReview.net.
- [4] Beatrice Bevilacqua, Moshe Eliasof, Eli Meir, Bruno Ribeiro, and Haggai Maron. 2024. Efficient Subgraph GNNs by Learning Effective Selection Policies. In *The Twelfth International Conference on Learning Representations*.
- [5] Beatrice Bevilacqua, Fabrizio Frasca, Derek Lim, Balasubramaniam Srinivasan, Chen Cai, Gopinath Balamurugan, Michael M. Bronstein, and Haggai Maron. 2022. Equivariant Subgraph Aggregation Networks. In *International Conference on Learning Representations*.
- [6] Filippo Maria Bianchi, Daniele Grattarola, and Cesare Alippi. 2020. Spectral clustering with graph neural networks for graph pooling. In *International conference on machine learning*. PMLR, 874–883.
- [7] Angela Bonifati, M Tamer Özsu, Yuanyuan Tian, Hannes Voigt, Wenyan Yu, and Wenjie Zhang. 2024. The future of graph analytics. In *Companion of the 2024 International Conference on Management of Data*. 544–545.
- [8] Cătălina Cangea, Petar Veličković, Nikola Jovanović, Thomas Kipf, and Pietro Liò. 2018. Towards sparse hierarchical graph classifiers. *arXiv preprint arXiv:1811.01287* (2018).
- [9] Tingyang Chen, Dazhuo Qiu, Yinghui Wu, Arijit Khan, Xiangyu Ke, and Yunjun Gao. 2024. View-based explanations for graph neural networks. *Proceedings of the ACM on Management of Data* 2 (2024), 1–27.
- [10] Zhengdao Chen, Lei Chen, Soledad Villar, and Joan Bruna. 2020. Can graph neural networks count substructures? *Advances in neural information processing systems* 33 (2020), 10383–10395.
- [11] Sara Cohen. 2016. Data management for social networking. In *Proceedings of the 35th ACM SIGMOD-SIGACT-SIGAI symposium on principles of database systems*. 165–177.
- [12] Gabriele Corso, Luca Cavalleri, Dominique Beaini, Pietro Liò, and Petar Veličković. 2020. Principal neighborhood aggregation for graph nets. *Advances in Neural Information Processing Systems* 33 (2020), 13260–13271.
- [13] Leonardo Cotta, Christopher Morris, and Bruno Ribeiro. 2021. Reconstruction for powerful graph representations. *Advances in Neural Information Processing Systems* 34 (2021), 1713–1726.
- [14] Yue Cui, Kai Zheng, Dingshan Cui, Jiandong Xie, Liwei Deng, Feiteng Huang, and Xiaofang Zhou. 2021. METRO: a generic graph neural network framework for multivariate time series forecasting. *Proceedings of the VLDB Endowment* 15 (2021), 224–236.
- [15] Gunduz Vehbi Demirci, Aparajita Haldar, and Hakan Ferhatosmanoglu. 2022. Scalable Graph Convolutional Network Training on Distributed-Memory Systems. *Proc. VLDB Endow.* 16 (2022), 711–724. <https://www.vldb.org/pvldb/vol16/p711-demirci.pdf>
- [16] Inderjit S Dhillon, Yuqiang Guan, and Brian Kulis. 2007. Weighted graph cuts without eigenvectors: a multilevel approach. *IEEE transactions on pattern analysis and machine intelligence* 29 (2007), 1944–1957.
- [17] Frederik Diehl. 2019. Edge contraction pooling for graph neural networks. *arXiv preprint arXiv:1905.10990* (2019).
- [18] Zhihao Ding, Jieming Shi, Shiqi Shen, Xuequn Shang, Jiannong Cao, Zhipeng Wang, and Zhi Gong. 2024. Sgood: Substructure-enhanced graph-level out-of-distribution detection. In *Proceedings of the 33rd ACM International Conference on Information and Knowledge Management*. 467–476.
- [19] Yuxiao Dong, Nitesh V Chawla, and Ananthram Swami. 2017. metapath2vec: Scalable representation learning for heterogeneous networks. In *Proceedings of the 23rd ACM SIGKDD international conference on knowledge discovery and data mining*. 135–144.
- [20] Vijay Prakash Dwivedi, Chaitanya K Joshi, Anh Tuan Luu, Thomas Laurent, Yoshua Bengio, and Xavier Bresson. 2023. Benchmarking graph neural networks. *Journal of Machine Learning Research* 24 (2023), 1–48.
- [21] Negin Entezari, Saba A Al-Sayouri, Amirali Darvishzadeh, and Evangelos E Papalexakis. 2020. All you need is low (rank) defending against adversarial attacks on graphs. In *Proceedings of the 13th international conference on web search and data mining*. 169–177.
- [22] Federico Errica, Marco Podda, Davide Bacciu, Alessio Micheli, et al. 2020. A Fair Comparison of Graph Neural Networks for Graph Classification. In *Proceedings of the Eighth International Conference on Learning Representations (ICLR 2020)*.
- [23] Wenfei Fan. 2022. Big graphs: challenges and opportunities. *Proceedings of the VLDB Endowment* 15 (2022), 3782–3797.
- [24] Yixiang Fang, Wensheng Luo, and Chenhao Ma. 2022. Densest subgraph discovery on large graphs: Applications, challenges, and techniques. *Proceedings of the VLDB Endowment* 15 (2022), 3766–3769.
- [25] Bahare Fatemi, Sami Abu-El-Haija, Anton Tsitsulin, Mehran Kazemi, Dustin Zelle, Neslihan Bulut, Jonathan Halcrow, and Bryan Perozzi. 2023. UGSL: A unified framework for benchmarking graph structure learning. *arXiv preprint arXiv:2308.10737* (2023).
- [26] Jiarui Feng, Yixin Chen, Fuhai Li, Anindya Sarkar, and Muhan Zhang. 2022. How powerful are k-hop message passing graph neural networks. *Advances in Neural Information Processing Systems* 35 (2022), 4776–4790.
- [27] Hendrik Fichtenberger and Pan Peng. 2022. Approximately Counting Subgraphs in Data Streams. In *Proceedings of the 41st ACM SIGMOD-SIGACT-SIGAI Symposium on Principles of Database Systems*. 413–425.

- [28] Luca Franceschi, Mathias Niepert, Massimiliano Pontil, and Xiao He. 2019. Learning discrete structures for graph neural networks. In *International conference on machine learning*. PMLR, 1972–1982.
- [29] Fabrizio Frasca, Beatrice Bevilacqua, Michael Bronstein, and Haggai Maron. 2022. Understanding and extending subgraph gnns by rethinking their symmetries. *Advances in Neural Information Processing Systems* 35 (2022), 31376–31390.
- [30] Hongyang Gao and Shuiwang Ji. 2019. Graph u-nets. In *international conference on machine learning*. PMLR, 2083–2092.
- [31] Shihong Gao, Yiming Li, Xin Zhang, Yanyan Shen, Yingxia Shao, and Lei Chen. 2024. SIMPLE: Efficient Temporal Graph Neural Network Training at Scale with Dynamic Data Placement. *Proceedings of the ACM on Management of Data* 2 (2024), 1–25.
- [32] Justin Gilmer, Samuel S Schoenholz, Patrick F Riley, Oriol Vinyals, and George E Dahl. 2017. Neural message passing for quantum chemistry. In *International conference on machine learning*. Pmlr, 1263–1272.
- [33] Aditya Grover and Jure Leskovec. 2016. node2vec: Scalable feature learning for networks. In *Proceedings of the 22nd ACM SIGKDD international conference on Knowledge discovery and data mining*. 855–864.
- [34] Rustam Guliyev, Aparajita Haldar, and Hakan Ferhatosmanoglu. 2024. D3-GNN: Dynamic Distributed Dataflow for Streaming Graph Neural Networks. *Proceedings of the VLDB Endowment* 17 (2024), 2764–2777.
- [35] Will Hamilton, Zhitao Ying, and Jure Leskovec. 2017. Inductive representation learning on large graphs. *Advances in neural information processing systems* 30 (2017).
- [36] Kaveh Hassani and Amir Hosein Khasahmadi. 2020. Contrastive multi-view representation learning on graphs. In *International Conference on Machine Learning*. PMLR, 4116–4126.
- [37] Taher Haveliwala. 1999. *Efficient computation of PageRank*. Technical Report. Stanford.
- [38] Zhenyu Hou, Xiao Liu, Yukuo Cen, Yuxiao Dong, Hongxia Yang, Chunjie Wang, and Jie Tang. 2022. Graphmae: Self-supervised masked graph autoencoders. In *Proceedings of the 28th ACM SIGKDD Conference on Knowledge Discovery and Data Mining*. 594–604.
- [39] Weihua Hu, Matthias Fey, Marinka Zitnik, Yuxiao Dong, Hongyu Ren, Bowen Liu, Michele Catasta, and Jure Leskovec. 2020. Open graph benchmark: Datasets for machine learning on graphs. *Advances in neural information processing systems* 33 (2020), 22118–22133.
- [40] Ziniu Hu, Yuxiao Dong, Kuansan Wang, Kai-Wei Chang, and Yizhou Sun. 2020. GPT-GNN: Generative pre-training of graph neural networks. In *Proceedings of the 26th ACM SIGKDD international conference on knowledge discovery & data mining*. 1857–1867.
- [41] Kezhao Huang, Haitian Jiang, Minjie Wang, Guangxuan Xiao, David Wipf, Xiang Song, Quan Gan, Zengfeng Huang, Jidong Zhai, and Zheng Zhang. 2024. FreshGNN: Reducing Memory Access via Stable Historical Embeddings for Graph Neural Network Training. *Proceedings of the VLDB Endowment* 17 (2024), 1473–1486.
- [42] Yinan Huang, Xingang Peng, Jianzhu Ma, and Muhan Zhang. 2022. Boosting the Cycle Counting Power of Graph Neural Networks with l2GNNs. *arXiv preprint arXiv:2210.13978* (2022).
- [43] IMDb 2024. IMDb: Ratings, Reviews, and Where to Watch the Best Movies & TV Shows – imdb.com. <https://www.imdb.com/>.
- [44] Eric Inae, Gang Liu, and Meng Jiang. 2023. Motif-aware attribute masking for molecular graph pre-training. *arXiv preprint arXiv:2309.04589* (2023).
- [45] Wei Jin, Tyler Derr, Haochen Liu, Yiqi Wang, Suhang Wang, Zitao Liu, and Jiliang Tang. 2020. Self-supervised learning on graphs: Deep insights and new direction. *arXiv preprint arXiv:2006.10141* (2020).
- [46] Wei Jin, Tyler Derr, Yiqi Wang, Yao Ma, Zitao Liu, and Jiliang Tang. 2021. Node similarity preserving graph convolutional networks. In *Proceedings of the 14th ACM international conference on web search and data mining*. 148–156.
- [47] Wei Jin, Yao Ma, Xiaorui Liu, Xianfeng Tang, Suhang Wang, and Jiliang Tang. 2020. Graph structure learning for robust graph neural networks. In *Proceedings of the 26th ACM SIGKDD international conference on knowledge discovery & data mining*. 66–74.
- [48] Thomas N Kipf and Max Welling. 2016. Semi-supervised classification with graph convolutional networks. *arXiv preprint arXiv:1609.02907* (2016).
- [49] Junhyun Lee, Inyeop Lee, and Jaewoo Kang. 2019. Self-attention graph pooling. In *International conference on machine learning*. pmlr, 3734–3743.
- [50] Namkyeong Lee, Junseok Lee, and Chanyoung Park. 2022. Augmentation-free self-supervised learning on graphs. In *Proceedings of the AAAI Conference on Artificial Intelligence*, Vol. 36. 7372–7380.
- [51] Haoyang Li and Lei Chen. 2021. Cache-based gnn system for dynamic graphs. In *Proceedings of the 30th ACM International Conference on Information & Knowledge Management*. 937–946.
- [52] Haoyang Li and Lei Chen. 2023. Early: Efficient and reliable graph neural network for dynamic graphs. *Proceedings of the ACM on Management of Data* 1 (2023), 1–28.
- [53] Haoyang Li, Shimin Di, Lei Chen, and Xiaofang Zhou. 2024. E2GCL: Efficient and Expressive Contrastive Learning on Graph Neural Networks. In *2024 IEEE 40th International Conference on Data Engineering (ICDE)*. IEEE, 859–873.
- [54] Haoyang Li, Shimin Di, Calvin Hong Yi Li, Lei Chen, and Xiaofang Zhou. 2024. Fight Fire with Fire: Towards Robust Graph Neural Networks on Dynamic Graphs via Actively Defense. *Proceedings of the VLDB Endowment* 17 (2024), 2050–2063.
- [55] Haoyang Li, Shimin Di, Zijian Li, Lei Chen, and Jiannong Cao. 2022. Black-box adversarial attack and defense on graph neural networks. In *2022 IEEE 38th International Conference on Data Engineering (ICDE)*. IEEE, 1017–1030.
- [56] Qiyan Li and Jeffrey Xu Yu. 2024. Fast Local Subgraph Counting. *Proceedings of the VLDB Endowment* 17 (2024), 1967–1980.
- [57] Yuanzhi Li and Yang Yuan. 2017. Convergence analysis of two-layer neural networks with relu activation. *Advances in neural information processing systems* 30 (2017).
- [58] Zhengdao Li, Yong Cao, Kefan Shuai, Yiming Miao, and Kai Hwang. 2024. Rethinking the effectiveness of graph classification datasets in benchmarks for assessing GNNs. *arXiv preprint arXiv:2407.04999* (2024).
- [59] Zhiyuan Li, Xun Jian, Yue Wang, and Lei Chen. 2022. CC-GNN: A community and contraction-based graph neural network. In *2022 IEEE International Conference on Data Mining (ICDM)*. IEEE, 231–240.
- [60] Zhiyuan Li, Xun Jian, Yue Wang, Yingxia Shao, and Lei Chen. 2024. DAHA: Accelerating GNN Training with Data and Hardware Aware Execution Planning. *Proc. VLDB Endow.* 17 (2024), 1364–1376.
- [61] Zhixun Li, Xin Sun, Yifan Luo, Yanqiao Zhu, Dingshuo Chen, Yingtao Luo, Xiangxin Zhou, Qiang Liu, Shu Wu, Liang Wang, et al. 2024. GSLB: the graph structure learning benchmark. *Advances in Neural Information Processing Systems* 36 (2024).
- [62] Zhixun Li, Liang Wang, Xin Sun, Yifan Luo, Yanqiao Zhu, Dingshuo Chen, Yingtao Luo, Xiangxin Zhou, Qiang Liu, Shu Wu, et al. 2023. Gslb: The graph structure learning benchmark. *Advances in Neural Information Processing Systems* 36 (2023), 30306–30318.
- [63] Ningyi Liao, Dingheng Mo, Siqiang Luo, Xiang Li, and Pengcheng Yin. 2022. SCARA: scalable graph neural networks with feature-oriented optimization. *Proceedings of the VLDB Endowment* 15 (2022), 3240–3248.
- [64] Qingyuan Linghu, Fan Zhang, Xuemin Lin, Wenjie Zhang, and Ying Zhang. 2020. Global reinforcement of social networks: The anchored coreness problem. In *Proceedings of the 2020 ACM SIGMOD International Conference on Management of Data*. 2211–2226.
- [65] Renjie Liu, Yichuan Wang, Xiao Yan, Haitian Jiang, Zhenkun Cai, Minjie Wang, Bo Tang, and Jinyang Li. 2025. DiskGNN: Bridging I/O efficiency and model accuracy for out-of-core GNN training. *Proceedings of the ACM on Management of Data* 3 (2025), 1–27.
- [66] Yucheng Liu, Zipeng Gao, Xiangyang Liu, Pengfei Luo, Yang Yang, and Hui Xiong. 2023. QTIAH-GNN: Quantity and topology imbalance-aware heterogeneous graph neural network for bankruptcy prediction. In *Proceedings of the 29th ACM SIGKDD Conference on Knowledge Discovery and Data Mining*. 1572–1582.
- [67] Dongsheng Luo, Wei Cheng, Wenchao Yu, Bo Zong, Jingchao Ni, Haifeng Chen, and Xiang Zhang. 2021. Learning to drop: Robust graph neural network via topological denoising. In *Proceedings of the 14th ACM international conference on web search and data mining*. 779–787.
- [68] Xiaoxiao Ma, Jia Wu, Jian Yang, and Quan Z Sheng. 2023. Towards graph-level anomaly detection via deep evolutionary mapping. In *Proceedings of the 29th ACM SIGKDD conference on knowledge discovery and data mining*. 1631–1642.
- [69] Debmalaya Mandal, Sourav Medya, Brian Uzzi, and Charu Aggarwal. 2022. Metalearning with graph neural networks: Methods and applications. *ACM SIGKDD Explorations Newsletter* 23 (2022), 13–22.
- [70] Diego Mesquita, Amauri Souza, and Samuel Kaski. 2020. Rethinking pooling in graph neural networks. *Advances in Neural Information Processing Systems* 33 (2020), 2220–2231.
- [71] Christopher Morris, Nils M Kriege, Franka Bause, Kristian Kersting, Petra Mutzel, and Marion Neumann. 2020. TUDataset: A collection of benchmark datasets for learning with graphs. *arXiv preprint arXiv:2007.08663* (2020).
- [72] Sarfaraz K Niazi and Zamara Mariam. 2023. Recent advances in machine-learning-based chemoinformatics: a comprehensive review. *International Journal of Molecular Sciences* 24 (2023), 11488.
- [73] Giannis Nikolentzos, George Dasoulas, and Michalis Vazirgiannis. 2020. K-hop graph neural networks. *Neural Networks* 130 (2020), 195–205.
- [74] Hakan T Otal, Abdulhamit Subasi, Furkan Kurt, M Abdullah Canbaz, and Yasin Uzun. 2024. Analysis of Gene Regulatory Networks from Gene Expression Using Graph Neural Networks. *arXiv preprint arXiv:2409.13664* (2024).
- [75] Pál András Papp, Karolis Martinkus, Lukas Faber, and Roger Wattenhofer. 2021. DropGNN: Random dropouts increase the expressiveness of graph neural networks. *Advances in Neural Information Processing Systems* 34 (2021), 21997–22009.
- [76] Pál András Papp and Roger Wattenhofer. 2022. A theoretical comparison of graph neural network extensions. In *International Conference on Machine Learning*. PMLR, 17323–17345.

- [77] Bryan Perozzi et al. 2014. Deepwalk: Online learning of social representations. In *Proceedings of the 20th ACM SIGKDD international conference on Knowledge discovery and data mining*. 701–710.
- [78] Chendi Qian, Gaurav Rattan, Floris Geerts, Mathias Niepert, and Christopher Morris. 2022. Ordered subgraph aggregation networks. *Advances in Neural Information Processing Systems* 35 (2022), 21030–21045.
- [79] Reddit. 2024. Reddit. <https://www.reddit.com/?rdt=55615>.
- [80] Dylan Sandfelder, Priyesh Vijayan, and William L Hamilton. 2021. Ego-gnns: Exploiting ego structures in graph neural networks. In *ICASSP 2021-2021 IEEE International Conference on Acoustics, Speech and Signal Processing (ICASSP)*. IEEE, 8523–8527.
- [81] Zezhi Shao, Zhao Zhang, Wei Wei, Fei Wang, Yongjun Xu, Xin Cao, and Christian S Jensen. 2022. Decoupled dynamic spatial-temporal graph neural network for traffic forecasting. *Proceedings of the VLDB Endowment* 15 (2022), 2733–2746.
- [82] Nino Shervashidze, SVN Vishwanathan, Tobias Petri, Kurt Mehlhorn, and Karsten Borgwardt. 2009. Efficient graphlet kernels for large graph comparison. In *Artificial intelligence and statistics*. PMLR, 488–495.
- [83] Zhen Song, Yu Gu, Tianyi Li, Qingsun, Yanfeng Zhang, Christian S Jensen, and Ge Yu. 2023. ADGNN: towards scalable GNN training with aggregation-difference aware sampling. *Proceedings of the ACM on Management of Data* 1 (2023), 1–26.
- [84] Li Sun, Zhenhao Huang, Zixi Wang, Feiyang Wang, Hao Peng, and S Yu Philip. 2024. Motif-aware riemannian graph neural network with generative-contrastive learning. In *Proceedings of the AAAI Conference on Artificial Intelligence*, Vol. 38. 9044–9052.
- [85] Qingyun Sun, Jianxin Li, Hao Peng, Jia Wu, Xingcheng Fu, Cheng Ji, and S Yu Philip. 2022. Graph structure learning with variational information bottleneck. In *Proceedings of the AAAI Conference on Artificial Intelligence*, Vol. 36. 4165–4174.
- [86] Shantanu Thakoor, Corentin Tallec, Mohammad Gheshlaghi Azar, Rémi Munos, Petar Veličković, and Michal Valko. 2021. Bootstrapped representation learning on graphs. In *ICLR 2021 Workshop on Geometrical and Topological Representation Learning*.
- [87] A Vaswani. 2017. Attention is all you need. *Advances in Neural Information Processing Systems* (2017).
- [88] Petar Veličković, Guillem Cucurull, Arantxa Casanova, Adriana Romero, Pietro Lio, and Yoshua Bengio. 2017. Graph attention networks. *arXiv preprint arXiv:1710.10903* (2017).
- [89] Daixin Wang, Peng Cui, and Wenwu Zhu. 2016. Structural deep network embedding. In *Proceedings of the 22nd ACM SIGKDD international conference on Knowledge discovery and data mining*. 1225–1234.
- [90] Guangtao Wang, Zhitao Ying, Jing Huang, and Jure Leskovec. 2021. Multi-hop Attention Graph Neural Network. In *International Joint Conference on Artificial Intelligence*.
- [91] Huizhao Wang, Yao Fu, Tao Yu, Linghui Hu, Weihao Jiang, and Shiliang Pu. 2023. Prose: Graph structure learning via progressive strategy. In *Proceedings of the 29th ACM SIGKDD Conference on Knowledge Discovery and Data Mining*. 2337–2348.
- [92] Haonan Wang, Jieyu Zhang, Qi Zhu, and Wei Huang. 2022. Augmentation-Free Graph Contrastive Learning. *arXiv preprint arXiv:2204.04874* (2022).
- [93] Kai Wang, Yuwei Xu, and Siquang Luo. 2024. TIGER: Training Inductive Graph Neural Network for Large-scale Knowledge Graph Reasoning. *Proceedings of the VLDB Endowment* 17 (2024), 2459–2472.
- [94] Pengyun Wang, Junyu Luo, Yanxin Shen, Ming Zhang, Siyu Heng, and Xiao Luo. 2024. A comprehensive graph pooling benchmark: Effectiveness, robustness and generalizability. *arXiv preprint arXiv:2406.09031* (2024).
- [95] Qiang Wang, Yao Chen, Weng-Fai Wong, and Bingsheng He. 2023. Hongtu: Scalable full-graph GNN training on multiple gpus. *Proceedings of the ACM on Management of Data* 1 (2023), 1–27.
- [96] Song Wang, Zhen Tan, Huan Liu, and Jundong Li. 2023. Contrastive meta-learning for few-shot node classification. In *Proceedings of the 29th ACM SIGKDD conference on knowledge discovery and data mining*. 2386–2397.
- [97] Yu Wang, Wei Jin, and Tyler Derr. 2022. Graph neural networks: Self-supervised learning. *Graph Neural Networks: Foundations, Frontiers, and Applications* (2022), 391–420.
- [98] Huijun Wu, Chen Wang, Yuriy Tyshetskiy, Andrew Docherty, Kai Lu, and Liming Zhu. 2019. Adversarial examples for graph data: deep insights into attack and defense. In *Proceedings of the 28th International Joint Conference on Artificial Intelligence*. 4816–4823.
- [99] Zonghan Wu, Shirui Pan, Fengwen Chen, Guodong Long, Chengqi Zhang, and Philip S Yu. 2020. A comprehensive survey on graph neural networks. *IEEE transactions on neural networks and learning systems* 32 (2020), 4–24.
- [100] Yongan Xiang, Zezhong Ding, Rui Guo, Shangyou Wang, Xike Xie, and S Kevin Zhou. 2025. Capsule: An Out-of-Core Training Mechanism for Colossal GNNs. *Proceedings of the ACM on Management of Data* 3 (2025), 1–30.
- [101] Keyulu Xu, Weihua Hu, Jure Leskovec, and Stefanie Jegelka. 2019. How Powerful are Graph Neural Networks?. In *7th International Conference on Learning Representations, ICLR 2019, New Orleans, LA, USA, May 6–9, 2019*. OpenReview.net. <https://openreview.net/forum?id=ryGs6iA5Km>
- [102] Zuoyu Yan, Junru Zhou, Liangcai Gao, Zhi Tang, and Muhan Zhang. 2024. An Efficient Subgraph GNN with Provably Substructure Counting Power. In *Proceedings of the 30th ACM SIGKDD Conference on Knowledge Discovery and Data Mining*. 3702–3713.
- [103] Kuo Yang, Zhengyang Zhou, Wei Sun, Pengkun Wang, Xu Wang, and Yang Wang. 2023. Extract and refine: Finding a support subgraph set for graph representation. In *Proceedings of the 29th ACM SIGKDD Conference on Knowledge Discovery and Data Mining*. 2953–2964.
- [104] Tianjun Yao, Yingxu Wang, Kun Zhang, and Shangsong Liang. 2023. Improving the expressiveness of k-hop message-passing gnns by injecting contextualized substructure information. In *Proceedings of the 29th ACM SIGKDD Conference on Knowledge Discovery and Data Mining*. 3070–3081.
- [105] Chun-Hsiao Yeh, Cheng-Yao Hong, Yen-Chi Hsu, Tyng-Luh Liu, Yubei Chen, and Yann LeCun. 2022. Decoupled contrastive learning. In *European conference on computer vision*. Springer, 668–684.
- [106] Zhitao Ying, Jiaxuan You, Christopher Morris, Xiang Ren, Will Hamilton, and Jure Leskovec. 2018. Hierarchical graph representation learning with differentiable pooling. *Advances in neural information processing systems* 31 (2018).
- [107] Jiaxuan You, Jonathan M Gomes-Selman, Rex Ying, and Jure Leskovec. 2021. Identity-aware graph neural networks. In *Proceedings of the AAAI conference on artificial intelligence*, Vol. 35. 10737–10745.
- [108] Jinliang Yuan, Hualei Yu, Meng Cao, Ming Xu, Junyuan Xie, and Chongjun Wang. 2021. Semi-Supervised and Self-Supervised Classification with Multi-View Graph Neural Networks. In *Proceedings of the 30th ACM International Conference on Information & Knowledge Management*. 2466–2476.
- [109] Xuan Zang, Xianbing Zhao, and Buzhou Tang. 2023. Hierarchical molecular graph self-supervised learning for property prediction. *Communications Chemistry* 6 (2023), 34.
- [110] Muhan Zhang and Pan Li. 2021. Nested graph neural networks. *Advances in Neural Information Processing Systems* 34 (2021), 15734–15747.
- [111] Xin Zhang, Yanyan Shen, Yingxia Shao, and Lei Chen. 2023. DUCATI: A dual-cache training system for graph neural networks on giant graphs with the GPU. *Proceedings of the ACM on Management of Data* 1 (2023), 1–24.
- [112] Zhen Zhang, Jiajun Bu, Martin Ester, Jianfeng Zhang, Chengwei Yao, Zhi Yu, and Can Wang. 2019. Hierarchical graph pooling with structure learning. *arXiv preprint arXiv:1911.05954* (2019).
- [113] Zaixi Zhang, Qi Liu, Hao Wang, Chengqiang Lu, and Chee-Kong Lee. 2021. Motif-based graph self-supervised learning for molecular property prediction. *Advances in Neural Information Processing Systems* 34 (2021), 15870–15882.
- [114] Lingxiao Zhao, Wei Jin, Leman Akoglu, and Neil Shah. 2022. From Stars to Subgraphs: Uplifting Any GNN with Local Structure Awareness. In *International Conference on Learning Representations*.
- [115] Lingxiao Zhao, Wei Jin, Leman Akoglu, and Neil Shah. 2022. From Stars to Subgraphs: Uplifting Any GNN with Local Structure Awareness. In *The Tenth International Conference on Learning Representations, ICLR 2022, Virtual Event, April 25–29, 2022*. OpenReview.net.
- [116] Zhou Zhiyao, Sheng Zhou, Bochao Mao, Xuanyi Zhou, Jiawei Chen, Qiaoyu Tan, Daochen Zha, Yan Feng, Chun Chen, and Can Wang. 2024. OpenGSL: A comprehensive benchmark for graph structure learning. *Advances in Neural Information Processing Systems* 36 (2024).
- [117] Zhiqiang Zhong and Davide Mottin. 2023. Knowledge-augmented Graph Machine Learning for Drug Discovery: From Precision to Interpretability. In *Proceedings of the 29th ACM SIGKDD Conference on Knowledge Discovery and Data Mining*. 5841–5842.
- [118] Zhiyao Zhou, Sheng Zhou, Bochao Mao, Jiawei Chen, Qingyun Sun, Yan Feng, Chun Chen, and Can Wang. 2024. Motif-driven Subgraph Structure Learning for Graph Classification. *arXiv preprint arXiv:2406.08897* (2024).
- [119] Yanqiao Zhu et al. 2021. Graph contrastive learning with adaptive augmentation. In *Proceedings of the Web Conference 2021*. 2069–2080.
- [120] Yanqiao Zhu, Yichen Xu, Feng Yu, Qiang Liu, Shu Wu, and Liang Wang. 2020. Deep graph contrastive representation learning. *arXiv preprint arXiv:2006.04131* (2020).
- [121] Yuanhang Zou, Zhihao Ding, Jieming Shi, Shuting Guo, Chunchen Su, and Yafei Zhang. 2023. EmbedX: A Versatile, Efficient and Scalable Platform to Embed Both Graphs and High-Dimensional Sparse Data. *Proceedings of the VLDB Endowment* 16 (2023), 3543–3556.